

SOLVING AC OPTIMAL POWER FLOW WITH DISCRETE DECISIONS TO GLOBAL OPTIMALITY

KEVIN-MARTIN AIGNER¹, ROBERT BURLACU^{1,2,3}, FRAUKE LIERS^{1,2},
AND ALEXANDER MARTIN^{1,2,3}

ABSTRACT. We present a solution framework for general alternating current optimal power flow (AC OPF) problems that include discrete decisions. The latter occur, for instance, in the context of the curtailment of renewables or the switching of power generation units and transmission lines. Our approach delivers globally optimal solutions and is provably convergent. We model AC OPF problems with discrete decisions as mixed-integer nonlinear programs. The solution method starts from a known framework that uses piecewise linear relaxations. These relaxations are modeled as mixed-integer linear programs and adaptively refined until some termination criterion is fulfilled. In this work, we extend and complement this approach by both problem-specific and very general algorithmic enhancements. In particular, they consist in mixed-integer second-order cone relaxations as well as primal and dual cutting planes. For example objective cuts and no-good-cuts help to compute good feasible solutions while outer approximation constraints tighten the relaxations.

We present extensive numerical results for various AC OPF problems where discrete decisions play a major role. Even for hard instances with a large proportion of discrete decisions, the method is able to generate high quality solutions efficiently. Furthermore, we compare our method with state-of-the-art MINLP solvers. Our method outperforms all other algorithms.

1. INTRODUCTION

In power system analysis, a main objective is the numerical evaluation and optimization of the power flow in an electricity network. The predominantly used model is the optimal power flow (OPF) problem. The basic version results in a continuous nonlinear optimization problem. The task is to compute an optimal generation and power transmission strategy with minimal costs. This optimization problem allows to plan future extensions of power supply grids and to establish optimal operating conditions for electricity systems. The current and future challenges of the transition towards renewable energy production can only be mastered through optimized decisions.

In this paper, we extend the classical OPF model of [12] by incorporating discrete decisions on a fairly general level. Discrete decisions are necessary, e.g., to model discrete feed-ins or the switching of power generation units and transmission lines. Typically, power generation units must generate a minimal (positive) amount of power and therefore cannot be controlled continuously from zero. One has to decide if a

Key words and phrases. Mixed-Integer Nonlinear Programming, Second-Order Cone Programming, Piecewise Linear Relaxation, Discrete Decisions, AC Optimal Power Flow, Generator Switching, Transmission Line Switching, Curtailment of Renewables.

generation unit is switched on or off. Optimal transmission switching is a paradigm that decides if lines are switched in and out of the network in order to maximize economic efficiency of generation dispatch. Discrete feed-ins can occur, for example, in the context of renewable energies. With the increasing share of renewable energy sources, their feed-in also has to be regulated in order to maintain network security and avoid line overload. Under the German Renewable Energy Sources Act (EEG), for instance, these curtailment options are realized in discrete steps within Germany. At the same time, the amount of curtailed power should be as small as possible to conserve resources and avoid potential compensation payments from network operators to the owner of production units. The additional component of integer decisions for the OPF thus provides the possibility to establish more comprehensive and realistic models. Such models are for example part of the prominent ARPA-E's Grid Optimization Competition [3], where the focus is to quickly find feasible solutions for very large real-world test instances. In contrast to this, we are interested in global approaches for discrete AC OPF problems, i.e., we equally aim for good primal solutions and tight dual bounds.

We consider an alternating current (AC) power flow model that is described by a system of non-convex nonlinear equations. This model was originally introduced by [12]. For a broad overview of the history of solving the AC OPF, we refer to [43]. The authors of [21] and [22] survey OPF literature to a great extent. AC OPF in its basic version is already a mathematically challenging problem, see [9]. More drastically, the inclusion of discrete decisions finally leads to mixed-integer nonlinear programs (MINLPs) that are in general NP-hard optimization problems and therefore very difficult to solve in practice. This is aggravated by the fact that many AC models contain trigonometric functions, which are not supported by every state-of-the-art MINLP solvers such as Baron ([51]) and SCIP ([42]).

We model such problems as MINLPs. To solve these, we start from the approach from [11] and incorporate several enhancements specific for AC OPF problems where discrete decisions play a major role. In [11], the authors use piecewise linear relaxations of the MINLP that are modeled as mixed-integer linear programs (MIPs). These MIPs are adaptively refined until a given termination criterion is fulfilled. Piecewise linear functions have been successfully used in the literature to construct tight relaxations for difficult nonlinear problems, see, e.g., [10, 18, 20, 29, 37, 38, 45, 52]. In this work, we extend this approach by known problem-specific relaxations that are based on second-order cone formulations. Combining this ingredient with the MIP-based piecewise linear relaxations results in mixed-integer second-order cone programs (MISOCPs) that yield tight dual bounds. Several enhancements together with the non-trivial combination of existing algorithmic approaches for obtaining sharp primal and dual bounds improve the algorithm further and deliver a practically efficient solution procedure. We prove that the convergence result from [11] is also applicable to our framework. In addition, extensive numerical results show the practicability of our method for various discrete AC OPF problems. Even for the very challenging instances that include the discrete curtailment of renewables our approach is able to deliver solutions of high quality.

Many of the global optimization approaches that have been developed for AC OPF in recent years use convex optimization like semi-definite programming (SDP).

Originally, the authors of [4] introduced the convex SDP relaxation of the AC OPF. It was shown that this relaxation together with a “rank 1” condition is equivalent to the AC OPF. Since the “rank 1” condition is up to now not algorithmically tractable, the quality of this convex relaxation can only be numerically verified. It also depends on the parameters of the power network and its topology. Consequently, the solution of the SDP relaxation may not always deliver satisfying results. For many instances, however, this relaxation performs very well and often leads to a global solution for the AC OPF. With the extended conic quadratic problem formulation of [32], one can easily obtain a second-order cone relaxation of the AC OPF. This relaxation is weaker than the SDP relaxation but needs less computational effort on average. In [36], this reformulation and the approach that uses the SDP problem are combined. The authors construct second-order cone programming (SOCP) relaxations that are embedded in a branch-and-cut framework. The authors of [41] further tighten quadratic relaxations with piecewise convex function relaxations. In [27], the SDP relaxation was sharpened with RLT-cuts and bound tightening. Additional cutting planes, convex envelopes, and further bound tightening techniques complete the approach yielding the current state-of-the-art solver for AC OPF. Moreover, in [15] the authors give an overview of different relaxations for AC OPF and present a comparison of their quality.

We point out that DC optimal power flow models, which are a linear approximation of AC models, have been studied to a large amount, see [14] for example. The benefit is that DC models bypass the nonlinear part of the AC model. Hence, very large power networks can be considered. This approximation is also suitable for problems where the OPF appears to be a subproblem. Common models where the DC approximation is predominantly used are, e.g., electricity market ([28, 54]) and chance constrained optimal power flow models ([2, 7]). For MIP techniques applied to network expansion problems, see [1]. However, for several electrical (distribution) networks, the DC approximation is not accurate enough. In [47] a thorough analysis is given for which power networks the DC approximation is suitable.

In general, the combination of AC OPF with discrete decisions has scarcely been addressed in the literature. In [5], the authors present a two-level approach for OPF with additional switching of the transmission lines of the power network. First, they compute optimal discrete decisions with a DC model and then derive feasible decisions from the DC solution with an AC model. The same problem is discussed in [34], where a method is proposed that utilizes mixed-integer SOCP relaxations. These are based on the SOCP relaxations for AC OPF that are introduced in [32]. The problem is solved in a branch-and-cut framework.

AC OPF problems with switching of the generator units appear to be even less studied in the literature. In his Ph.D. thesis [39], the author develops heuristic solutions for this problem. Recently, [48] have proposed a mixed-integer method. Based on a mixed-integer SDP relaxation of the problem, they derive two MIP approximations that are subsequently solved: an inner and an outer MIP approximation. The inner MIP approximation improves feasible solutions, whereas the outer MIP approximation delivers a relaxation and therefore a dual bound.

A more special class of OPF problems with discrete decisions are the time-dependent unit commitment OPF problems. They are often decomposed in a discrete master problem and an continuous AC OPF subproblem. The drawback here, however, is

that the AC OPF subproblem can often not be solved to global optimality; see for example [13, 23, 40]. Moreover, we refer to [49], where an overview of the solution methods for unit commitment problems that have been developed in recent decades is given.

The key contributions of our work are:

AC OPF with Discrete Decisions: We combine solution approaches from the literature into an algorithmic framework that can handle discrete decisions for AC OPF on a fairly general level. Our approach is able to incorporate any discrete decisions that can be represented in algebraic form using integer variables.

Globally Convergent Solution Approach: We extend and complement the adaptive construction of piecewise linear relaxations by both problem-specific (like MISOCP relaxations and DC OPF heuristics) and general algorithmic enhancements (like no-good-cuts and outer approximation cuts). Although these enhancements are known in the literature on their own, the novelty of our method is to combine them in a way that leads to a significant speed-up for piecewise linear relaxation based solution approaches. We obtain an efficient algorithm for discrete AC OPF problems that delivers globally optimal solutions. We extend the theoretical results from [11] and prove that our approach converges to the global optimal solution of the MINLP problem with an increasing accuracy of the piecewise linear relaxations.

Computational Results: We provide a computational study based on benchmark instances from the NESTA test case archive ([16]). Our approach is able to generate high quality solutions efficiently together with tight dual bounds. It outperforms state-of-the-art MINLP solvers for various MINLP instances that result from transmission line and generator switching and the discrete curtailment of renewables.

This article is organized as follows. In Section 2, recall how to formulate the AC OPF problem as a nonlinear program. Starting from this, we develop MINLP models for different scenarios that include discrete decisions in Section 3. Section 4 describes the solution framework and shows its convergence. Finally, we present comprehensive computational results in Section 5 and conclude this work in Section 6.

2. THE AC OPF MODEL

In this section, we describe the NLP model for the AC OPF problem. It is based on the power flow models from [32]. Section 3 completes it to an MINLP model with integer formulations that include the various discrete decisions.

We represent a power network by an undirected graph $N = (B, L)$, where the node set B denotes the buses and the edge set L the transmission lines. The subset $U \subseteq B$ contains the nodes with a generator. Our objective is to minimize the production costs of the generators and to simultaneously satisfy all physical and technical constraints. The physical restrictions are essentially described by Ohm's and Kirchhoff's Law. The technical restrictions represent the limits of the transmission lines and of the production quantities of the generators.

The power supply system is characterized by a complex nodal admittance matrix $Y \in \mathbb{C}^{|B| \times |B|}$ that describes the nodal admittance of the buses. Roughly speaking, this matrix contains information about the network topology and transmission parameters. To each transmission line $(k, l) \in L$, we assign a component $Y_{kl} = G_{kl} + iH_{kl}$. The shunt conductance and susceptance are denoted by g_{kk} and h_{kk} , respectively for

every bus $k \in B$. As in [36] and [31], we follow the standard notation and denote by p_k^g and q_k^g the real and reactive power output of the generator that is associated to the bus $k \in U$ and assume lower and upper bounds $(p_k^g)^-, (q_k^g)^-$ and $(p_k^g)^+, (q_k^g)^+$ to be given. For a network node without generation units $k \in B \setminus U$, we set $p_k^g = 0$ and $q_k^g = 0$. We point out that there are instances with more than one generator on a bus. More than one line between two nodes are also possible. In this cases, we simply duplicate the corresponding bus and line in the sets B and L and label them with increasing sub-indices. Usually the AC OPF minimizes production costs. The objective is a univariate linear or convex quadratic function in dependence of active power generation

$$C_k(p_k^g) := C_{k,1}(p_k^g)^2 + C_{k,2}p_k^g + C_{k,3} \quad (1)$$

with given constants $C_{k,1} \geq 0$ and $C_{k,2}, C_{k,3} \in \mathbb{R}$ for every generator node $k \in U$. The corresponding power demand at bus k is given by p_k^d and q_k^d . Moreover, we denote the real and reactive power on a transmission line $(k, l) \in L$ sent from node $k \in B$ to $l \in \delta(k)$ by p_{kl} and q_{kl} , respectively, where $\delta(k)$ denotes the set of neighbor nodes for k .

In the literature, there are different formulations for the AC OPF depending on the form the complex voltage on a network node is described. Recently, [8] has provided a broad overview of different OPF formulations. We want to highlight that each problem formulation has its own advantages and disadvantages and not all of them are equivalent. The two equivalent polar formulation and the extended conic quadratic formulation specify the complex voltage by voltage magnitude and voltage angle. The power flow equations are described by trigonometric functions in these formulations. Alternatively, the rectangular formulation specifies the complex voltage by its real and imaginary part. This model avoids trigonometric expressions.

For our purposes, the extended conic quadratic formulation is the most appropriate since it contains the fewest nonlinear expressions and thus introduces the least complexity for an approach based on piecewise linear relaxations of the nonlinearities. In this paper, we therefore focus on the extended conic quadratic formulation introduced by [32], for which, additionally, convex SOCP-relaxations can be easily derived. Please note that we also incorporate the rectangular formulation for a comparison of our approach with state-of-the-art MINLP solvers. For more details on the modeling in this alternative problem formulation, we refer to Appendix 8.

2.1. Extended Conic Quadratic Formulation. The complex voltage on a bus $k \in B$ is given by $V_k = u_k(\cos \theta_k + i \sin \theta_k)$, where $u_k = |V_k|$ is the voltage magnitude with lower and upper bounds $|V_k|^-$ and $|V_k|^+$, and θ_k is the phase angle. In [32] the variable substitutions

$$c_{kk} := u_k^2, \quad c_{kl} := u_k u_l \cos(\theta_k - \theta_l), \quad t_{kl} := -u_k u_l \sin(\theta_k - \theta_l) \quad (2)$$

are used for each bus $k \in B$ and line $(k, l) \in L$ and the extended conic quadratic AC OPF flow model is formulated as

$$\min_{p^g, q^g, c, t, \theta, p, q} \sum_{k \in U} C_k(p_k^g) \quad (3a)$$

$$s.t. \quad p_k^g - p_k^d = g_{kk}(c_{kk}) + \sum_{l \in \delta(k)} p_{kl} \quad \text{for all } k \in B, \quad (3b)$$

$$q_k^g - q_k^d = -h_{kk}(c_{kk}) + \sum_{l \in \delta(k)} q_{kl} \quad \text{for all } k \in B, \quad (3c)$$

$$p_{kl} = -G_{kl}(c_{kk} - c_{kl}) - H_{kl}t_{kl} \quad \text{for all } (k, l) \in L, \quad (3d)$$

$$q_{kl} = H_{kl}(c_{kk} - c_{kl}) - G_{kl}t_{kl} \quad \text{for all } (k, l) \in L, \quad (3e)$$

$$c_{kl}^2 + t_{kl}^2 = c_{kk}c_{ll} \quad \text{for all } (k, l) \in L, \quad (3f)$$

$$\theta_l - \theta_k = \arctan2(t_{kl}, c_{kl}) \quad \text{for all } (k, l) \in L. \quad (3g)$$

$$c_{kl} = c_{lk}, \quad t_{kl} = -t_{lk} \quad \text{for all } (k, l) \in L, \quad (3h)$$

$$p_{kl}^2 + q_{kl}^2 \leq (d_{kl}^+)^2 \quad \text{for all } (k, l) \in L, \quad (3i)$$

$$(p_k^g)^- \leq p_k^g \leq (p_k^g)^+ \quad \text{for all } k \in U, \quad (3j)$$

$$(q_k^g)^- \leq q_k^g \leq (q_k^g)^+ \quad \text{for all } k \in U, \quad (3k)$$

$$(|V_k|^-)^2 \leq c_{kk} \leq (|V_k|^+)^2 \quad \text{for all } k \in B, \quad (3l)$$

$$\theta_{kl}^- \leq \theta_k - \theta_l \leq \theta_{kl}^+ \quad \text{for all } (k, l) \in L, \quad (3m)$$

$$p^g, q^g \in \mathbb{R}^{|U|}, \quad \theta \in \mathbb{R}^{|B|}, \quad c \in \mathbb{R}^{|B|+|L|}, \quad t, p, q \in \mathbb{R}^{|L|}. \quad (3n)$$

The constraints (3b) and (3c) guarantee the conservation of active and reactive power at the buses of the network. Commonly, the real and reactive power flow p_{kl} and q_{kl} are described as in (3d) and (3e). Additionally, we bound the apparent power d_{kl} on line $(k, l) \in L$ by d_{kl}^+ . Since $d_{kl}^2 = p_{kl}^2 + q_{kl}^2$, we ensure this restriction by (3i). We point out that one of the variables θ_k is set to zero at a reference node. The nonlinear part of the AC OPF model (3) is (3f)–(3g) and (3i).

Finally, we remark that $-\pi/2 < \theta_l - \theta_k < \pi/2$ holds in practice for a lot of test instances. Under this assumption, we can reformulate the discontinuous constraint (3g) by

$$c_{kl} \tan(\theta_l - \theta_k) = t_{kl}. \quad (4)$$

The latter is much easier to handle than (3g) because of the discontinuity of the two-argument arcus tangent. If there are no bounds on the voltage angle differences or if they are not small enough, we can replace (3g) by

$$c_{kl} \sin(\theta_l - \theta_k) = t_{kl} \cos(\theta_l - \theta_k). \quad (5)$$

2.2. SOCP Relaxation of the Extended Conic Quadratic Formulation. As pointed out in [33, 35], we can easily obtain a SOCP relaxation of (3) by dropping constraint (3g) and substituting (3f) with

$$c_{kl}^2 + t_{kl}^2 \leq c_{kk}c_{ll} \quad \text{for all } (k, l) \in L. \quad (6)$$

The constraints (6) denote SOCP cones that are the convex hulls of (3f). We will use this relaxation in our solution framework to obtain tight dual bounds for the AC OPF problem (3).

3. EXTENSION TO DISCRETE DECISIONS

In this section, we show how to extend the NLP model from Section 2 to an MINLP for several scenarios that contain discrete decisions. We focus on the extended conic quadratic formulation (3).

3.1. Transmission Line Switching. Let $s_{kl}^t \in \{0, 1\}$ denote the switching status of a transmission line $(k, l) \in L$. The switching constraints of a line can be modeled by

$$p_{kl} = (-G_{kl}(c_{kk} - c_{kl}) - H_{kl}t_{kl})s_{kl}^t, \quad (7a)$$

$$q_{kl} = (H_{kl}(c_{kk} - c_{kl}) - G_{kl}t_{kl})s_{kl}^t, \quad (7b)$$

$$(c_{kl}^2 + t_{kl}^2 - c_{kk}c_{ll})s_{kl}^t = 0, \quad (7c)$$

$$(c_{kl} \tan(\theta_l - \theta_k) - t_{kl})s_{kl}^t = 0 \quad (7d)$$

for all $(k, l) \in L$. Equation (7a) and (7b) guarantees that the power flow on line $(k, l) \in L$ is set to zero if the line is switched off. The nonlinear constraints (3f)–(3g) are only active if the transmission edge is switched on. This is achieved by (7c) and (7d).

The model (7) contains several products of continuous and binary variables. In order to reduce the number of such bilinear products, we follow [34] and instead introduce additional variables $\tilde{c}_{kl} := c_{kk}s_{kl}^t$ for every line $(k, l) \in L$ and model the transmission switching via

$$p_{kl} = -G_{kl}(\tilde{c}_{kl} - c_{kl}) - H_{kl}t_{kl}, \quad (8a)$$

$$q_{kl} = H_{kl}(\tilde{c}_{kl} - c_{kl}) - G_{kl}t_{kl}, \quad (8b)$$

$$c_{kl}^2 + t_{kl}^2 = \tilde{c}_{kl}\tilde{c}_{lk}, \quad (8c)$$

$$c_{kl} \tan(\theta_l - \theta_k) = t_{kl}, \quad (8d)$$

$$\tilde{c}_{kl} = c_{kk}s_{kl}^t, \quad (8e)$$

$$c_{kl}^- s_{kl}^t \leq c_{kl} \leq c_{kl}^+ s_{kl}^t, \quad (8f)$$

$$t_{kl}^- s_{kl}^t \leq t_{kl} \leq t_{kl}^+ s_{kl}^t \quad (8g)$$

for every transmission line $(k, l) \in L$. The parameters c_{kl}^- , c_{kl}^+ and t_{kl}^- , t_{kl}^+ denote the lower and upper bounds for the decision variables c_{kl} and t_{kl} for all lines $(k, l) \in L$. These bounds are not initially stated in problem (2) and usually not part of given input parameters. We can use in (8f)–(8g) the trivial bounds

$$c_{kl}^- = -|V_k|^+ |V_l|^+, \quad c_{kl}^+ = |V_k|^+ |V_l|^+ \\ t_{kl}^- = -|V_k|^+ |V_l|^+, \quad t_{kl}^+ = |V_k|^+ |V_l|^+.$$

It is easy to verify that (7) and (8) are equivalent.

The MINLP model for AC OPF with transmission line switching can be obtained by exchanging (3d)–(3g) with (8) and introducing the additional variables $s^t \in \{0, 1\}^{|L|}$ and $\tilde{c}_{kl} \geq 0$ for all lines $(k, l) \in L$.

3.2. Generator Switching. In order to integrate the switching status of a generator, we introduce the binary variable $s_k^g \in \{0, 1\}$ for every generator bus $k \in U$. We model the switching of a generator with

$$s_k^g (p_k^g)^- \leq p_k^g \leq s_k^g (p_k^g)^+, \quad (10a)$$

$$s_k^g (q_k^g)^- \leq q_k^g \leq s_k^g (q_k^g)^+. \quad (10b)$$

These constraints ensure that both active and reactive power generation are set to zero if the power production is switched off. Otherwise, the active and reactive generator feed-in is continuously controllable inside the bounds.

Because there are no cost associated to switched-off production units, we change the objective function (1) for the AC OPF with generator switching to

$$\sum_{k \in U} \left(C_{k,1} (p_k^g)^2 + C_{k,2} p_k^g + C_{k,3} s_k^g \right).$$

We receive the MINLP model for generator switching by exchanging the already mentioned objective function, constraints (3j)–(3k) with (10a)–(10b) and binary variables $s^g \in \{0, 1\}^{|U|}$.

3.3. Curtailment of Renewables. In practice, the feed-in from renewables is often regulated in discrete steps. We denote with $U^c \subseteq B$ the nodes with power injection from renewables. If necessary, the feed-in is curtailed to a certain percentage of the installed active power capacity $p_k^{\text{inst}} \geq 0$, for every node $k \in U^c$, that is the intended full-load sustained energy production. To do this, we introduce discrete decision variables $s_k^c \in \mathcal{S}_k^c \subseteq [0, 1]$, $k \in U^c$, which we refer to as curtailment factors from the discrete set \mathcal{S}_k^c of curtailment options. In practice, sets with few discrete levels are common. Typical steps are for example $\{0, 0.3, 0.6, 1\}$ or $\{0, 0.1, \dots, 0.9, 1\}$. At a node $k \in U^c$, the active power fed into the network cannot exceed $s_k^c p_k^{\text{inst}} \in [0, p_k^{\text{inst}}]$. Any feed-in above this value is cut off.

As in [2], we model this by

$$p_k^{c,\text{in}} = \min(p_k^c, s_k^c p_k^{\text{inst}}) = \begin{cases} p_k^c & \text{if } p_k^c \leq s_k^c p_k^{\text{inst}}, \\ s_k^c p_k^{\text{inst}} & \text{else,} \end{cases} \quad (11)$$

where $p_k^c \geq 0$ denotes the active power production from renewables on node $k \in U^c$ and $p_k^{c,\text{in}} \in [0, p_k^c]$ the (curtailed) active power from renewables fed into the network. This minimum expression could be linearized by introducing auxiliary mixed-integer variables and linear constraints. As the active power production from renewables is a constant input parameter in our setting, we can avoid dealing with minimum terms in (11). Therefore, we compute the possible absolute curtailment options

$$p_k^{c,\text{in}} \in \{ \min(p_k^c, s_k^c p_k^{\text{inst}}) : s_k^c \in \mathcal{S}_k^c \} \quad (12)$$

and integrate them in the model as the sum of auxiliary binaries with special ordered set constraints (of type 1).

We assume a constant power factor $\cos(\phi) \in (0, 1]$ for the feed-in such that the reactive power is given by

$$q_k^{c,\text{in}} = \sqrt{\frac{1 - \cos(\phi)^2}{\cos(\phi)^2}} p_k^{c,\text{in}}. \quad (13)$$

Since the disposal of renewable energy should be avoided and may also lead to compensation payments for the electricity network operators, the amount of curtailed active power must be penalized in the objective function. We replace the objective function in (3) by

$$\sum_{k \in U} \left(C_{k,1} (p_k^g)^2 + C_{k,2} p_k^g + C_{k,3} \right) + \sum_{k \in U^c} C_k^c (p_k^c - p_k^{c,\text{in}}), \quad (14)$$

where the constant $C_k^c \geq 0$ is the cost coefficient assigned to curtailment costs. Here, we assume linear costs to obtain again a univariate convex quadratic objective function.

This also coincides with the pricing of compensation costs through curtailment in practice. For an abbreviated notation, let $p_k^{c,\text{in}} = 0$ for all nodes $k \in B \setminus U^c$. We integrate the curtailment model in the AC OPF by exchanging (3b) and (3c) with

$$\begin{aligned} p_k^g + p_k^{c,\text{in}} - p_k^d &= g_{kk}(c_{kk}) + \sum_{l \in \delta(k)} p_{kl}, \\ q_k^g + q_k^{c,\text{in}} - q_k^d &= -h_{kk}(c_{kk}) + \sum_{l \in \delta(k)} q_{kl}, \end{aligned}$$

together with (12)–(13) for all nodes $k \in B$.

Remark 3.1 (MISOCP Relaxation). *As in Section 2.2, we can relax the nonlinearities analogously to construct a convex relaxation for the nonlinear parts of each extended model. Due to the appearance of discrete variables this relaxation forms an MISOCP, which can be solved by standard software. This is integrated in our solution approach by adding the SOCP constraints to the piecewise linear MIP relaxations.*

4. SOLUTION FRAMEWORK

Our goal is to obtain globally optimal solutions for AC OPF with discrete decisions. Most global approaches for AC OPF use some sort of relaxations in combination with a local NLP solver, where convergence to the global optimal solution is not always guaranteed. The situation becomes even more challenging if we include integral variables.

4.1. The Algorithm. We consider the method proposed in [11] and improved in [10], where MINLPs are solved to global optimality by solving a series of MIPs. The main idea is to use piecewise linear functions to construct MIP relaxations of the underlying MINLP. Then, an algorithm is developed to find a global optimum by iteratively solving these relaxations, which are adaptively refined. Algorithm 1 gives a schematic overview of the approach, which is also applicable for solving general MINLPs.

The main benefit of using relaxations is that we can embed this procedure into a primal-dual approach. Whenever a relaxation is infeasible, we can immediately conclude that the MINLP itself is infeasible because of the relaxation property. Moreover, any dual objective bound of an MIP relaxation delivers a dual objective bound for the MINLP problem.

At the same time, MIP relaxations preserve the discrete structure of the MINLP, since only the nonlinear part is relaxed. This is exploited as follows: Whenever a feasible solution of an MIP relaxation is found, all discrete variables of the MINLP are fixed according to the respective solution of the MIP relaxation. Solving the resulting NLP to local optimality delivers feasible solutions for the MINLP in many cases. This heuristic is contained in Step (2)-(ii) of Algorithm 1. For problems where the discrete decisions strongly affect the overall difficulty, the preservation of the discrete structure is very advantageous in the course of finding integer-feasible solutions. This is mainly due to the fact that the discrete part of the problem is tackled by mature MIP technology. It has been demonstrated in [11] and [10] in the context of gas network optimization. We are therefore confident to build our approach on the same solution framework, as we are interested in globally optimal solutions for AC OPF with (potentially difficult) discrete decisions.

Algorithm 1: Adaptive MIP-based algorithm for solving MINLPs

Input: An MINLP problem P with continuous nonlinearities and bounded variables, a run time limit T , and parameters ϵ_0 , ϵ_{final} , ϵ_{gap} and n_{glob} .
Output: If P is feasible, the algorithm returns an optimal solution of an MIP relaxation of P with an accuracy of ϵ_{final} or terminates if the time limit T is reached.

(1) Initialization:

Construct an initial MIP relaxation Π_0 of P using piecewise linear relaxations of the nonlinearities with an accuracy of ϵ_0 .

Main Loop: ($i \leftarrow -1$),

repeat

$i \leftarrow i + 1$

(2) Solve Relaxation:

(i) **if** $i \equiv 0 \pmod{n_{\text{glob}}}$ **then**

Solve Π_i to global optimality with optimal solution x^* .

else

Solve Π_i with relative gap $(\text{PB} - \text{DB})/(2\text{PB})$, if primal and dual bounds PB and DB are available, or ϵ_{gap} otherwise.

Denote the best found solution by x^* .

end

(ii) For each found solution x_i of Π_i fix all discrete variables of P according to x_i .

Solve the resulting NLPs to local optimality.

Construct feasible solutions for P from the solutions of the NLPs.

(3) Refine Relaxation:

Construct Π_{i+1} by refining the piecewise linear relaxations of the nonlinearities on the segments that contain the best found solution x^* of Π_i .

until The global optimal solution x^* of Π_i ($i \equiv 0 \pmod{n_{\text{glob}}}$) has accuracy ϵ_{final} or run time limit T is reached.

The piecewise linear relaxations are modeled with the help of the well-known incremental method. In this work, we focus on this method because it is known that the corresponding models can be optimized efficiently in practice, see [17, 25] and again [11]. However, there is a variety of MIP-based models for piecewise linear relaxations. A detailed overview is given by [53].

For a continuous one-dimensional function $f: [\bar{x}_0, \bar{x}_n] \rightarrow \mathbb{R}$, $x \mapsto y := f(x)$, we model a piecewise linear approximation of f with linearization points (\bar{x}_i, \bar{y}_i) as

$$x = \bar{x}_0 + \sum_{i=1}^n (\bar{x}_i - \bar{x}_{i-1}) \delta_i, \quad (16a)$$

$$y = \bar{y}_0 + \sum_{i=1}^n (\bar{y}_i - \bar{y}_{i-1}) \delta_i, \quad (16b)$$

$$0 \leq \delta_i \leq 1 \quad \text{for } i = 1, \dots, n, \quad (16c)$$

$$z_i \geq \delta_{i+1} \quad \text{for } i = 1, \dots, n-1, \quad (16d)$$

$$z_i \leq \delta_i \quad \text{for } i = 1, \dots, n-1, \quad (16e)$$

$$z_i \in \{0, 1\} \quad \text{for } i = 1, \dots, n-1. \quad (16f)$$

Constraints (16d) and (16e) ensure that the δ -variables satisfy the filling condition, which states that if $\delta_i > 0$ then $\delta_{i-1} = 1$ must hold. This means that δ_i can only be positive if for all previous $j = 1, \dots, i-1$ the variables δ_j are equal to one.

Let $\epsilon_u(f, i)$ be the maximum underestimation and $\epsilon_o(f, i)$ the maximum overestimation of f by the piecewise linear approximation on the segment $[\bar{x}_{i-1}, \bar{x}_i]$. Then, we obtain a piecewise linear relaxation of f by simply replacing (16b) with

$$y = \bar{y}_0 + \sum_{i=1}^n (\bar{y}_i - \bar{y}_{i-1}) \delta_i + e,$$

while $e \in \mathbb{R}$ and adding the inequalities

$$\begin{aligned} \epsilon_u(f, 1) + \sum_{i=1}^{n-1} z_i (\epsilon_u(f, i+1) - \epsilon_u(f, i)) &\geq e, \\ -\epsilon_o(f, 1) - \sum_{i=1}^{n-1} z_i (\epsilon_o(f, i+1) - \epsilon_o(f, i)) &\leq e. \end{aligned}$$

For results concerning the computation of the approximation errors $\epsilon_u(f, i)$, $\epsilon_o(f, i)$, and a generalization of this model to higher dimensions, we again refer to [11]. As we will see below, in our case, we only need the modeling for one-dimensional functions.

In the following, we present some algorithmic extensions to Algorithm 1 and give an overview of the enhanced method afterwards, which partially contains problem specific extensions.

4.2. Algorithmic Enhancements. Algorithm 1 is applicable for solving MINLPs to global optimality. To improve computing time and quality of solutions various extensions like adding valid cutting planes, presolve strategies, and heuristics are at hand. We group these in problem-specific and general valid enhancements, which we discuss first. In the following paragraphs, we also explain if and how the approaches can be applied for more general problem classes.

4.2.1. Preprocessing: Bound Tightening. The number of segments required to achieve a certain approximation quality in the linearization of nonlinear terms usually increases strongly with the domain size.

Before entering the main loop in Algorithm 1, we use the root relaxation of the initial MIP relaxation Π_0 and exchange its objective with the minimization or maximization of the variable we want to tighten. The resulting linear problems can be efficiently solved to global optimality and the optimal objective value of these auxiliary problems deliver often tight variable bounds, see [26]. This and similar known bound tightening procedures can be applied for general optimization problems. In the concrete context

of AC OPF, we choose to tighten the bounds of c_{kl} , s_{kl} and $\theta_k - \theta_l$. These variables are part of the nonlinear expressions and therefore tighter bounds have a large impact on the overall problem.

4.2.2. Univariate Reformulation of Bivariate Terms. One of the most common nonlinearities are a bivariate product xy with continuous variables x and y . A bivariate relaxation of $f(x, y) = xy$ requires a two-dimensional triangulation of the domain of f . To counteract the curse of dimensionality, we exploit the equality

$$xy = \frac{1}{2}((x + y)^2 - x^2 - y^2)$$

and substitute each term xy in our MINLP model with $\frac{1}{2}(z^2 - x^2 - y^2)$ and add the linear constraint $z = x + y$. Thus, we now only have univariate terms in our model. We strengthen the piecewise linear relaxation of these univariate nonlinearities by adding the well-known linear McCormick inequalities [44]

$$\begin{aligned} \frac{1}{2}(\tilde{z} - \tilde{x} - \tilde{y}) &\geq x^-y + xy^- - x^-y^-, \\ \frac{1}{2}(\tilde{z} - \tilde{x} - \tilde{y}) &\geq x^+y + xy^+ - x^+y^+, \\ \frac{1}{2}(\tilde{z} - \tilde{x} - \tilde{y}) &\leq x^+y + xy^- - x^+y^-, \\ \frac{1}{2}(\tilde{z} - \tilde{x} - \tilde{y}) &\leq xy^+ + x^-y - x^-y^+, \end{aligned}$$

where $\tilde{z} = z^2$, $\tilde{x} = x^2$, $\tilde{y} = y^2$ and x^-, y^- and x^+, y^+ again denote the lower and upper bounds of the variables x, y .

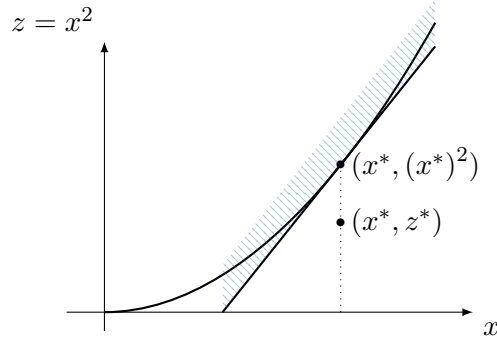
The univariate reformulation in combination with the McCormick inequalities can be applied for any nonlinear optimization problem including bilinear products. Preliminary computations on AC OPF instances show that for a given approximation accuracy for xy , the univariate reformulation yields a piecewise linear relaxation that requires significantly less binary variables than the bivariate formulation. Hence, the MISOCP relaxations in our algorithm have a smaller number of binary variables, while the tightness remains of the same quality.

4.2.3. Lower Linear Cutting Plane for Quadratic Terms. Another very common nonlinearity in optimization models are one dimensional quadratic expressions $z = x^2$. If the solution of a piecewise linear relaxation underestimates this constraint, we can introduce a lower linear cutting plane to strengthen the relaxation instead of subdividing a segment of the piecewise linear relaxation. We assume that the best found solution of relaxation Π_i in Step (2) of Algorithm 1 underestimates constraint $z = x^2$, i.e., $z^* < (x^*)^2$. Instead of refining the linear relaxation by adding a linearization point for Π_{i+1} , we introduce the linear cutting plane

$$z \geq 2x^*(x - x^*) + (x^*)^2.$$

This new constraint ensures that the current MIP solution is not feasible for the refined relaxation Π_{i+1} and therefore cut off, see Figure 1. Hereby, a strengthening of the relaxation can be achieved without further break points in the linearization. This

FIGURE 1. A lower linear cutting plane (dashed set) that separates a solution that underestimates $z = x^2$ from the feasible region.



avoids the introduction of an additional binary variable for the relaxation. This is applicable for all nonlinear models with quadratic expressions.

4.2.4. Refine Until Solution Is Cut Off. In the refinement Step (3) of Algorithm 1 it is not guaranteed that the best found MIP solution x^* is cut off in further iterations. In order to strengthen the refined MIP relaxation Π_{i+1} , we continue refining the piecewise linear relaxations on the corresponding segments until x^* is infeasible for the next iteration. This refinement strategy is applicable for any nonlinear model.

4.2.5. Primal Heuristic: No-good Cuts. Inspired by [34], we incorporate the classical no-good cuts into our algorithm, see [6] and [46]. Let S be the set of all binary decision variables. For a binary solution $s^* \in \{0, 1\}^{|S|}$ that shall be cut off, we obtain the corresponding no-good cut by

$$\sum_{\{i:s_i^*=1\}} (1 - s_i) + \sum_{\{i:s_i^*=0\}} s_i \geq 1.$$

First, we use these cuts to strengthen the primal heuristic that is already proposed in Step (2)-(ii) of Algorithm 1. In this step, we utilize the discrete part of all found MIP solutions in order to obtain MINLP solutions with the help of a local NLP solver. Initially, the algorithm starts with a rather coarse MIP relaxation of accuracy ϵ_0 . Thus, for a specific assignment s^* of the discrete variables, the first relaxations have a much larger feasible set of the continuous variables than the MINLP. It turns out that in numerous cases, s^* is feasible for these MIP relaxations, although it is infeasible for the MINLP. As a consequence, many refinement steps are necessary until s^* is excluded in the subsequent MIP relaxations. By adding no-good cuts, we can avoid unfavorable binary solutions at an earlier stage. As a drawback, however, we risk to cut off optimal solutions. Therefore, the optimal objective of a relaxation that includes no-good cuts provides no longer a valid dual bound for the original problem. In order to preserve the correctness of the approach, we omit these cuts in every n_{glob} th iteration, i.e., only the iterations $i \not\equiv 0 \pmod{n_{\text{glob}}}$ contain no-good cuts. This heuristic in combination with a local search algorithm can be applied for general mixed-integer nonlinear optimization problems.

4.2.6. *Tight Dual Bounds.* For many AC OPF instances the problem specific SOCP relaxation described in Subsection 2.2 delivers very strong, and sometimes even optimal, dual bounds ([32]). We therefore extend the MIP relaxations in our algorithm by adding the constraints (6) and solve the resulting MISOCPs to global optimality. In most cases the benefit of these tighter bounds outweighs the additional complexity of the (convex) SOCPs.

Similar to [11], we solve a MISOCP relaxation with a large but fixed number of linearization points in parallel to the main algorithm. Although this problem may not be solved within a reasonable run time, the dual bounds we obtain while solving the MISOCP also yield dual bounds for the original discrete AC OPF problem. In some cases, however, the high accuracy MISOCP relaxation is solved to optimality. Hence, we solve a series of such large MISOCP relaxations with an increasing approximation accuracy of the piecewise linear functions. In contrast to the main algorithm, where in each iteration we only refine locally some segments to keep the relaxations computationally more tractable, we now refine simultaneously at each segment of the piecewise linear relaxations. The solution of relaxations with high approximation accuracy can deliver tight dual bound and is applicable for general optimization problems.

4.2.7. *Outer Approximation of Transmission Limits.* Constraints (3i) are convex quadratic and the set

$$D_{kl} := \{(p_{kl}, q_{kl}) \in \mathbb{R}^2 \mid p_{kl}^2 + q_{kl}^2 \leq (d_{kl}^+)^2\}$$

is convex for all transmission lines $(k, l) \in L$. More precisely, the set describes the closed circular disk with the origin as center and radius $d_{kl}^+ > 0$.

Instead of constructing piecewise linear relaxations for these nonlinear constraints in Π_0 , we choose a discrete subset of vectors

$$(p_{kl}^j, q_{kl}^j)_{j \in J} \subseteq \{(p_{kl}, q_{kl}) \in \mathbb{R}^2 \mid p_{kl}^2 + q_{kl}^2 = (d_{kl}^+)^2\}$$

with index set $J \subseteq \mathbb{N}$ and use them for a linear outer approximation

$$\bigcap_{j \in J} \{(p_{kl}, q_{kl}) \in \mathbb{R}^2 \mid p_{kl}^j p_{kl} + q_{kl}^j q_{kl} \leq (d_{kl}^+)^2\}$$

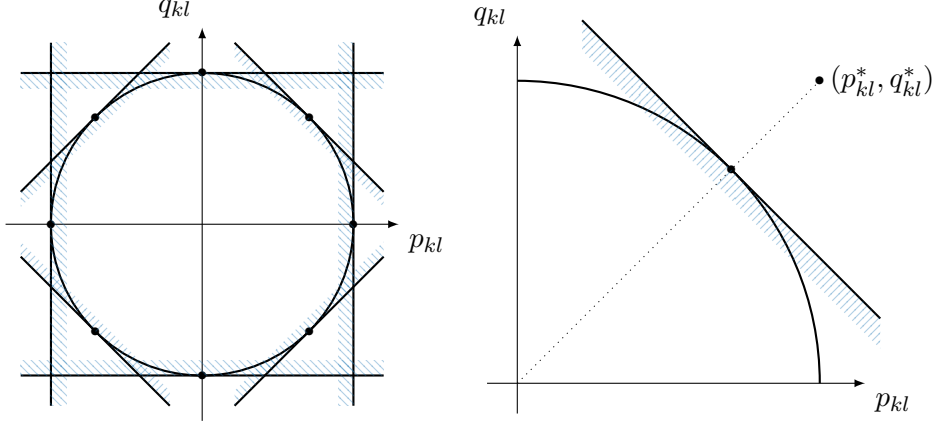
of D_{kl} . Figure 2 shows exemplarily the linear outer approximation with equidistantly chosen approximations points.

The refinement of the linear outer approximation can be easily incorporated in Step (3) of Algorithm 1. In case the best found solution of MIP Π_i is not feasible for the transmission limit (3i), i.e., $(p_{kl}^*)^2 + (q_{kl}^*)^2 > (d_{kl}^+)^2$ for some line $(k, l) \in L$, we construct a refined MIP relaxation Π_{i+1} by adding

$$p_{kl}^* p_{kl} + q_{kl}^* q_{kl} \leq \sqrt{(p_{kl}^*)^2 + (q_{kl}^*)^2} (d_{kl}^+)^2$$

to the existing linear outer approximation cutting planes of Π_i . In general, such valid linear inequalities can be derived for all problems with single convex constraints.

FIGURE 2. Outer approximation with eight equidistantly chosen approximations points (left) and refinement procedure for infeasible points (right), where a linear cutting plane separates (p_{kl}^*, q_{kl}^*) from the feasible region.



4.2.8. *Primal Heuristic: DC OPF.* As an additional problem-specific heuristic, we use the well-known approximative DC model to generate candidate solutions for the AC model that can be used as starting points for local search algorithms. This approximation assumes fixed voltage magnitudes and small phase angle differences in the network. The reactive part of electrical power is neglected and removed from the model. The corresponding nonlinear terms in the AC OPF are approximated by

$$\begin{aligned} |V_k| &\approx 1, \\ \sin(\theta_k - \theta_l) &\approx \theta_k - \theta_l, \\ \cos(\theta_k - \theta_l) &\approx 1, \end{aligned}$$

see [14] for details. In particular, in model (3), we remove (3c), (3e)–(3g) and (3k). Additionally, we impose the constraints

$$\begin{aligned} c_{kk} &= 1 \quad \forall k \in B, \\ c_{kl} &= 1 \quad \forall (k, l) \in L, \\ t_{kl} &= \theta_l - \theta_k \quad \forall (k, l) \in L. \end{aligned}$$

Transmission limits (3i) are replaced by

$$p_{kl} \leq d_{kl}^+, \quad p_{kl} \geq -d_{kl}^+ \quad \forall (k, l) \in L.$$

The resulting MIP is much easier to solve and often preserves the discrete structure of the discrete AC OPF problem such that a DC solution provides a feasible assignment of binaries for a local nonlinear solver. We can therefore utilize the same scheme as in Step (2)-(ii) of Algorithm 1 and use DC solutions for the construction of NLPs to local optimality. Furthermore, we solve a series of DC MIPs that we construct by iteratively adding no-good cuts for all found feasible DC solutions.

4.2.9. *Primal Heuristic: Curtailment of Renewables.* In case of curtailment of renewables, we include problem-specific primal cutting planes with the goal of obtaining high-quality feasible solutions quickly. Let \hat{x} be an incumbent MINLP solution. The idea is to add constraints inside a primal heuristic that temporarily enforce larger feed-ins from renewables than in the solution \hat{x} , i.e., a lower curtailment of the feed-ins.

With \hat{x} , we calculate for all nodes with discrete curtailment $k \in U^c \subseteq B$ the minimal amount of additionally injectable feed-in $\Delta \hat{p}_k^{c,\text{in}} := \min\{p_k^{c,\text{in}} - \hat{p}_k^{c,\text{in}} : p_k^{c,\text{in}} > \hat{p}_k^{c,\text{in}}\}$. The discrete steps of $p_k^{c,\text{in}}$ are defined in (12). Adding the constraints

$$\sum_k p_k^{c,\text{in}} \geq \sum_k \hat{p}_k^{c,\text{in}} + \min_{k \in U^c} \Delta \hat{p}_k^{c,\text{in}}, \quad (17a)$$

$$\sum_k p_k^{c,\text{in}} \leq \sum_k \hat{p}_k^{c,\text{in}} + \max_{k \in U^c} \Delta \hat{p}_k^{c,\text{in}}, \quad (17b)$$

help to find the “next best” solution as a lower curtailment leads to a better objective.

Please note that the constraints (17) lead to a smaller search space. As a result, feasible solutions can be found more quickly. The downside is that the global optimum might be cut off temporarily as constraint (17b) limits a higher feed-in from renewables. However, we omit these constraints in each iteration $i \equiv 0 \pmod{n_{\text{glob}}}$, which again enables us to find the global optimum of the MINLP and guarantees the correctness of the approach.

4.2.10. *The Enhanced Algorithm.* Algorithm 2 incorporates all previously mentioned extensions to Algorithm 1.

4.3. **Convergence Result.** Finally, we prove that Algorithm 2 is both correct and convergent. We first show that the following convergence result from [11] is applicable to our framework.

Definition 4.1. *The refinement procedure in Algorithm 1 is called δ -precise, if for an arbitrary sequence $S^i \in \mathcal{T}_i$ of simplices that are refined by the refinement procedure with initial triangulation \mathcal{T}_0 of D_f and given $\delta > 0$, there exists an index $N \in \mathbb{N}$ such that*

$$\text{diam}(S^N) < \delta$$

holds, whereby $\text{diam}(S^N) := \sup_{x', x'' \in S^N} \{\|x' - x''\|\}$.

Proposition 4.2 (Theorem 3.6, [11]). *If the refinement procedure in Algorithm 1 is δ -precise for every $\delta > 0$ and $T = \infty$, then Algorithm 1 is correct and terminates after a finite number of steps.*

As in [11], we use the classical longest-edge bisection as refinement procedure in Algorithm 2, which is shown to be δ -precise for every $\delta > 0$. The refinement of a simplex by the longest-edge bisection adds a linearization point in the middle of the longest side face. In the one-dimensional case this reduces to the center of an interval.

There are two main ingredients for the proof of Proposition 4.2: the continuity of the nonlinear functions f of the underlying MINLP and the compactness of their corresponding domains D_f .

Observation 4.3. *All variables in every (discrete) AC OPF problem are bounded. The nonlinear functions of the underlying MINLP are continuous and their domains are compact.*

Algorithm 2: Adaptive MISOCP-based algorithm for discrete AC OPF

Input: A discrete AC OPF problem P , a relative optimality gap ϵ_{opt} , a run time limit T , and parameters ϵ_0 , ϵ_{gap} , n_{DC} and n_{glob} .

Output: A feasible solution of P with optimality gap below ϵ_{opt} or termination if the time limit T is reached.

(0) Primal DC-based Heuristic:

for $k = 1$ **to** n_{DC} **do**

Solve the discrete DC OPF approximation Ω_i of P from Section 4.2.8.

For each found feasible solution x_i of Ω_i fix all discrete variables of P according to x_i and add a discrete no-good-cut for x_i to Ω_{i+1} .

Solve the resulting NLPs to local optimality.

Construct feasible solutions for P from the solutions of the NLPs.

end

(1) Initialization:

Construct an initial MIP relaxation Π_0 of P using piecewise linear relaxations of the nonlinearities with an accuracy of ϵ_0 .

Main Loop: ($i \leftarrow -1$)

repeat

$i \leftarrow i + 1$

(2) Solve Relaxation:

(i) **if** $i \equiv 0 \pmod{n_{\text{glob}}}$ **then**

Construct an MISOCP relaxation $\tilde{\Pi}_i$ of P by adding the constraints (6) to Π_i .

Solve $\tilde{\Pi}_i$ to global optimality with optimal solution x^* .

else

Add a discrete no-good-cut for each vector in the set C_{NG} to Π_i and curtailment constraints as in (17) corresponding to the incumbent MINLP solution.

Solve Π_i with relative gap $(\text{PB} - \text{DB})/(2\text{PB})$, if primal and dual bounds PB and DB are available, or ϵ_{gap} otherwise.

Denote the best found solution by x^* .

end

(ii) For each found feasible solution x_i of Π_i fix all discrete variables of P according to x_i .

Solve the resulting NLPs to local optimality.

Construct feasible solutions for P from the solutions of the NLPs.

Add x_i to the set C_{NG} of no-good-cut solutions for the next iteration.

(3) Refine Relaxation:

Construct Π_{i+1} by refining the piecewise linear relaxations of the nonlinearities on the segments that contain the best found solution x^* of Π_i .

until Relative optimality gap is below ϵ_{opt} or run time limit T is reached.

The nonlinearities are stated in constraints (3a), (3f), (3g) and (3i). As in (9), we can derive trivial bounds for the variables c_{kl}, t_{kl} for all $(k, l) \in L$ that have no bounds. The same holds for the active and reactive power flow on line $(k, l) \in L$ with trivial bounds

$$\begin{aligned} p_{kl}^- &:= -d_{kl}^+, & p_{kl}^+ &:= d_{kl}^+, \\ q_{kl}^- &:= -d_{kl}^+, & q_{kl}^+ &:= d_{kl}^+. \end{aligned}$$

As discussed in Section 2.1, we replace the discontinuous constraint (3g) by (4) or (5) based on the given bounds for the voltage angle difference $\theta_k - \theta_l$ on transmission line $(k, l) \in L$. These constraints contain continuous nonlinearities. Since all variables are bounded, every nonlinear expression has a compact domain.

Therefore, Proposition 4.2 directly translates to Algorithm 2. Precisely speaking, however, the original version of Algorithm 1 does not deliver a global optimal solution for the underlying MINLP problem. It only guarantees to find a global optimal solution of an MIP relaxation with a (nonlinear) feasibility tolerance of ϵ_{final} .

With the following supplementary contribution to the convergence results from [11], we also obtain convergence of our approach to a global optimal solution. We state the result for Algorithm 1, since it directly translates to Algorithm 2.

Theorem 4.4. *Let the refinement procedure in Algorithm 1 (as in [11]) be δ -precise for every $\delta > 0$. If ϵ_{final} tends to zero and $T = \infty$, then the global optimal solution obtained by Algorithm 1 converges to a global optimal solution of the MINLP problem P iff P is feasible.*

Proof. Proof. First, it is clear that if Algorithm 1 converges to an optimal solution of the MINLP problem P , then P must be feasible.

Let us now assume that P is feasible. Then, any MIP relaxation of P is feasible. We consider a sequence $(\epsilon_{\text{final}}/2^i)$ of constantly decreasing final approximation accuracies with limit 0. For each of these sequence elements, we obtain a global optimal solution of an MIP relaxation that satisfies the corresponding approximation accuracy due to the δ -preciseness of the refinement procedure and Proposition 4.2. This yields a sequence of global optimal solutions (x^i) of some MIP relaxations that meet the approximation accuracy $\epsilon_{\text{final}}/2^i$. Under the assumption that the domain D_f is compact for each nonlinear function f of the underlying MINLP, there is a convergent subsequence of (x^i) with a limit \tilde{x} and a corresponding approximation accuracy of 0. Consequently, \tilde{x} is feasible for P , because the approximation error is 0 and P is feasible. Moreover, \tilde{x} is the global optimal solution of an MIP relaxation of P , from which it directly follows that \tilde{x} is global optimal for P due to the relaxation property. \square

The proof in Theorem 4.4 works equivalently if we use MISOCP relaxations instead of MIP relaxations of the underlying MINLP, which is a discrete AC OPF problem in our case. With the longest-edge bisection as refinement procedure, the continuity of the nonlinear functions f of a discrete AC OPF problem and the compactness of their corresponding domains D_f , and Theorem 4.4, we can finally conclude:

Corollary 4.5. *Algorithm 2 is both correct and convergent.*

5. NUMERICAL RESULTS

In this section, we present numerical results that demonstrate the applicability of Algorithm 2 for the discrete AC OPF problems from Section 3. We address the mentioned discrete AC OPF problems by running Algorithm 2 on all 20 instances of the NESTA benchmark set (v0.7.0) with up to 300 buses, see [16]. These instances are subdivided into three operating conditions: standard, active power increase (API), and small angle difference (SAD). This results in a total amount of 59 instances, since for the case “nеста_case_6_ww” no active power increase instance is given. We compare the results of our approach to [31] and [34] in case of transmission line switching.

All computations are carried out using a Python implementation of Algorithm 2 on a cluster using 4 cores of a machine with two Xeon E3-1240 v6 “Kaby Lake” chips (4 cores, HT disabled) running at 3.7 GHz with 32 GB of RAM. The run time limit is set to 2 hours for each instance with a global relative optimality gap of 0.01 %. We utilize Gurobi 9.0.2 as MIP/MISOCP solver, see [30], and CONOPT3 within GAMS 33.2.0, see [24].

We use the following abbreviations in the subsequent computations:

- IG: Initial Gap,
- FG: Final Gap,
- #LO: Number of lines that are switched off,
- #GO: Number of generators that are switched off,
- CT: Total amount of curtailed feed-in (percentage of produced solar power),
- T: run time in seconds.

We refer the (relative) initial gap (IG) to the optimality gap that we compute using the current best MINLP solution and the dual bound obtained after solving the first MISOCP relaxation $\tilde{\Pi}_0$ in Step (2)-(i) of Algorithm 2. The (relative) optimality gap reported at the end of our method is called final gap (FG). We calculate the (relative) optimality gap via

$$\text{GAP} = \frac{|\text{PB} - \text{DB}|}{\text{PB}}, \quad (18)$$

with PB as the objective value of the best found MINLP solution and DB the dual bound. If our method was not able to find a feasible solution we report ‘no sol’. If the test case is proven infeasible, we report ‘infeas’. The number of switched off transmission lines and generators in the best found solution of the algorithm is denoted by #LO and #GO. For instances that include the discrete curtailment, we compute the percentage of lost power (CT) with

$$\text{CT} = \frac{\sum_{k \in U^c} (p_k^c - p_k^{c,\text{in}})}{\sum_{k \in U^c} p_k^c}.$$

5.1. Transmission Line Switching. The discrete AC OPF problem that is mostly addressed in the literature is transmission line switching. Table 1 illustrates the results of our method for the transmission line switching problem from Section 3.1 performed on the NESTA instances.

Our approach solves 19 out of 59 instances to global optimality, while 37 instances have a proven gap below 1 %. On average, we obtain for the final optimality gap 1.54 % as arithmetic and 0.17 % as geometric mean. Strong MISOCP relaxations are a crucial

TABLE 1. Results summary for the transmission line switching AC OPF.

nesta_case_	standard				API				SAD			
	IG (%)	FG (%)	#LO	T (s)	IG (%)	FG (%)	#LO	T (s)	IG (%)	FG (%)	#LO	T (s)
3_lmbd	1.45	0.01	0	18.82	0.86	0.01	0	20.26	0.56	0.01	0	15.75
4_gs	0.01	0.01	0	5.64	0.64	0.01	0	70.42	6.04	0.01	0	4 881.25
5_pjm	1.13	0.01	1	2 770.82	0.05	0.01	1	87.50	3.58	0.01	0	328.95
6_ww	0.09	0.01	2	224.11					0.14	0.01	2	58.87
6_c	0.02	0.01	1	98.24	0.34	0.01	0	233.42	0.47	0.60	0	289.92
9_wscc	0.14	0.01	0	114.94	0.03	0.01	0	32.17	0.74	0.01	0	328.07
14_ieee	0.11	0.02	0	7 194.81	0.82	0.66	2	7 235.85	0.10	0.01	0	1 291.44
24_ieee_rts	0.02	0.01	0	7 173.88	7.32	4.12	5	7 260.81	3.51	2.44	4	7 225.63
29_edin	0.12	0.10	8	7 027.07	0.20	0.20	26	7 005.76	25.42	23.68	8	7 287.59
30_as	0.37	0.11	0	6 699.55	1.58	0.89	6	7 283.88	5.53	0.45	1	7 296.34
30_ieee	13.78	8.56	3	7 269.63	0.93	0.40	1	7 163.83	8.51	1.84	2	7 201.71
30_fsr	1.62	0.17	0	3 436.42	2.46	0.05	3	6 540.46	1.67	0.07	3	7 044.20
39_epri	0.05	0.01	2	7 212.06	1.44	0.40	2	7 163.55	0.05	0.02	2	7 295.66
57_ieee	0.07	0.07	6	7 236.72	0.12	0.12	6	7 204.03	0.06	0.06	3	6 614.83
73_ieee_rts	0.26	0.03	0	7 222.82	6.50	1.63	5	7 227.85	3.51	1.93	15	7 205.45
89_pegase	0.28	0.28	0	6 956.26	19.02	1.26	15	7 210.44	0.30	0.18	14	6 757.23
118_ieee	1.86	1.77	12	7 299.19	9.59	9.59	26	6 784.67	3.42	3.31	30	7 203.02
162_ieee_dtc	3.77	3.75	3	7 251.04	1.04	1.04	10	7 208.36	4.76	4.74	0	7 236.49
189_edin	2.22	2.22	29	7 260.39	3.16	3.16	0	7 200.22	2.57	2.57	27	6 802.37
300_ieee	2.97	2.96	0	7 230.80	no sol.	2.22	26	7 231.40	2.98	2.87	0	7 232.54

factor. In most cases, the initial MISOCP relaxations and consequently the initial gaps IG are already very tight. This coincides with observations from the literature, see for example [34].

The previously mentioned publication [31] and the authors of [34] also cover the transmission line switching problem. We compare our results by computing the average gap via the arithmetic and geometric mean. The number of instances that are considered in all three papers is 14. Please note that hardware, software and time limit are different across the compared approaches. For instance, in [31] a time limit of 10h and in [34] an iteration limit of 5 is used, while we impose a time limit of 2h.

TABLE 2. Comparison of average optimality gaps with [34] and [31] for optimal transmission switching

	arithmetic mean	geometric mean
Our Method	1.18%	0.18%
[34]	1.21%	0.22%
[31]	1.48%	0.62%

In Table 2 it can be seen that our approach delivers optimality gaps that are slightly better than [34]. In comparison with [31], the results are even more convincing. The difference between the two columns can be explained by a few outliers with a higher optimality gap. This is due to fact that the classic (MI)SOCP relaxation is not tight for these instances and more linearization points for the piecewise linear relaxation are required to obtain a tighter relaxation. In summary, our algorithm is very competitive in case of transmission line switching.

5.2. Generator Switching. The NESTA instances are in their current version not suitable for the generator switching problem of Section 3.2. In most of the cases the active power production minimum $(p_k^g)^-$ on a generator bus $k \in U$ is zero or very low.

The same holds for the reactive power. This means that it is not necessary to switch off a generator for these instances and the discrete variables have no effect on the AC OPF. To overcome this issue, we set the lower bounds for active power production as

$$(p_k^g)^- = 0.20(p_k^g)^+ \quad \text{for all } k \in U.$$

A lower bound of 20% is a common minimum production value of various power stations, e.g., gas or nuclear power plants. Different settings and even individual ones are also possible. Higher minimum power value would lead to more infeasible test cases.

As we can see in Table 3, we are able to solve 17 out of 59 instances to global optimality. Five test cases are proven infeasible. In total, 37 instances have a proven gap below 1%. On average, we obtain for the final optimality gap 2.63% as arithmetic and 0.19% as geometric mean. Again in many cases, the initial MISOCP relaxations together with the current best solution are already of high quality. However, there are some instances for which our approach reduces the optimality gap during computation significantly.

TABLE 3. Results summary for the generator switching AC OPF.

nesta_case_	standard				API				SAD			
	IG (%)	FG (%)	#GO	T (s)	IG (%)	FG (%)	#GO	T (s)	IG (%)	FG (%)	#GO	T (s)
3_lmbd	infeas.	infeas.	0	2.44	0.96	0.01	0	18.82	infeas.	infeas.	0	2.38
4_gs	0.01	0.01	0	3.85	0.64	0.01	0	57.52	1.54	0.01	0	19.01
5_pjm	14.47	0.14	1	7 235.03	0.27	0.01	0	320.07	1.43	0.01	0	103.28
6_ww	0.92	0.01	0	106.20					0.75	0.01	0	50.42
6_c	infeas.	infeas.	0	4.80	0.34	0.01	0	248.21	infeas.	infeas.	0	4.56
9_wscc	0.44	0.01	0	69.57	0.03	0.01	0	25.10	0.80	0.01	0	215.15
14_ieee	0.11	0.01	0	548.46	1.27	0.34	0	7 219.52	0.10	0.01	0	168.49
24_ieee_rts	0.02	0.01	11	7 293.27	8.78	0.92	14	7 233.12	5.18	0.80	8	7 234.73
29_edin	0.10	0.07	30	7 061.30	0.34	0.27	5	7 249.70	27.27	7.83	15	7 175.87
30_as	0.93	0.02	0	7 279.68	4.55	1.56	0	7 116.31	6.02	0.51	0	7 131.89
30_ieee	8.17	0.46	0	7 277.53	0.88	0.71	0	7 183.99	3.52	0.44	0	7 157.63
30_fsr	1.96	0.24	0	7 244.99	42.53	25.67	1	7 215.95	1.86	0.08	0	7 221.89
39_epri	0.06	0.01	0	7 208.01	2.57	0.42	0	7 137.72	0.09	0.01	0	4 065.54
57_ieee	0.07	0.05	0	7 198.66	0.21	0.11	0	7 029.47	0.06	0.03	0	7 052.60
73_ieee_rts	0.87	0.06	34	7 228.94	9.72	9.50	25	7 156.30	8.87	6.12	22	7 111.63
89_pegase	0.17	0.17	0	7 130.29	21.21	21.21	3	7 077.96	0.16	0.13	0	7 206.14
118_ieee	2.42	1.36	5	7 014.05	45.12	42.55	0	7 001.44	7.65	3.25	4	6 666.54
162_ieee_dtc	3.91	3.75	1	7 202.97	1.50	1.31	0	7 157.84	4.64	4.49	0	7 206.84
189_edin	1.96	1.96	14	7 121.85	infeas.	infeas.	0	836.96	2.16	2.16	15	6 902.23
300_ieee	1.33	1.29	5	7 241.52	0.76	0.76	10	7 244.15	1.31	1.29	5	7 235.38

5.3. Discrete Curtailment. The test cases from the NESTA archive do not contain power generation with discrete curtailment steps. In order to test the model from Section 3.3, we add on every second network node, i.e., on each node with an odd ID number, feed-in from renewables, e.g., solar or wind. Consequently, we obtain $|U^c| = \lceil 0.5|B| \rceil$. At the remaining network nodes, we set the income from renewables to zero. The input parameters for the additional power production consist of the installed capacity p_k^{inst} , the produced active power p_k^c , and the discrete curtailment steps \mathcal{S}_k that are available for all nodes $k \in U^c$. To compute the reactive power, we assume a constant power ratio $\cos(\phi)$ and define

$$p_k^{\text{inst}} = \frac{2.5 \sum_{k \in B} p_k^d}{|U^c|}, \quad p_k^c = 0.8 p_k^{\text{inst}}, \quad \mathcal{S}_k = \{0, 0.3, 0.6, 1\}, \quad \cos(\phi) = 0.9,$$

for every bus $k \in U^c$. Other relevant combinations of p^{inst} (from 1.0 to 3.0) and p^c deliver characteristically very similar results. The assumption that $p^c = 0.8p^{\text{inst}}$ simulates solar energy production during a sunny day in the summer. We want to point out that values for the installed capacity smaller than one times or greater than three times the total demand lead in most cases to no or a complete curtailment of renewables.

For the inclusion of curtailment costs, we set in (14) the cost factor

$$C_k^c = \frac{\sum_{k \in U} C_{k,1}(p^*)^2 + C_{k,2}p^* + C_{k,3}}{|U^c|}, \quad p^* := \frac{\sum_{k \in U^c} p_k^c}{|U|}.$$

In this way, we achieve that the curtailment costs are approximately as high as the production costs for the total amount of produced power from renewables distributed to all generators.

Table 4 shows the results for the discrete curtailment. Our approach solves 15 out of 59 instances to global optimality. In total, 15 instances have a proven gap below 1% and 30 below 10%. On average, we obtain for the final optimality gap 13.79% as arithmetic and 2.19% as geometric mean. These problems turn out to be more difficult to solve than generator and transmission line switching.

TABLE 4. Results summary for the discrete curtailment AC OPF.

nesta_case_	standard				API				SAD			
	IG (%)	FG (%)	CT (%)	T (s)	IG (%)	FG (%)	CT (%)	T (s)	IG (%)	FG (%)	CT (%)	T (s)
3_lmbd	12.97	0.01	62.50	28.02	0.12	0.01	62.50	12.47	12.61	0.01	62.50	18.01
4_gs	0.01	0.01	50.00	5.34	0.01	0.01	62.50	5.21	0.62	0.01	62.50	25.00
5_pjm	0.01	0.01	50.00	16.57	12.54	0.01	75.00	72.26	22.54	0.01	62.50	76.19
6_ww	6.13	0.01	87.50	12.47					0.02	0.01	87.50	7.56
6_c	22.21	5.61	50.01	7 273.25	17.59	0.01	50.00	151.65	17.25	0.01	50.01	222.73
9_wscc	3.07	1.65	55.00	7 196.19	1.76	0.01	50.00	394.64	3.04	0.01	55.00	860.95
14_ieee	23.99	22.50	60.71	7 252.48	14.27	14.20	50.00	7 228.97	21.78	18.06	60.71	7 246.31
24_ieee_rts	4.17	3.53	67.71	7 126.82	4.69	3.43	58.33	7 258.87	4.79	2.75	69.79	7 265.80
29_edin	11.45	8.68	50.00	7 154.62	5.94	5.33	70.83	7 285.59	7.96	7.95	55.83	7 291.79
30_as	17.07	11.73	70.00	7 171.89	38.66	9.67	58.33	7 192.10	16.21	6.72	70.83	7 250.70
30_ieee	17.54	14.82	50.00	7 238.05	24.75	21.22	54.17	7 280.28	17.38	15.37	50.83	7 273.68
30_fsr	28.28	19.44	50.84	7 281.09	29.88	19.54	55.00	7 209.06	52.75	9.59	51.67	7 228.73
39_epri	31.19	19.36	69.37	7 256.95	2.36	1.85	51.25	7 133.33	33.54	27.23	81.25	7 097.50
57_ieee	51.83	43.30	77.15	7 293.96	54.83	53.10	96.55	7 284.55	42.09	39.34	91.81	7 097.30
73_ieee_rts	5.25	4.55	68.92	7 061.84	24.43	19.16	76.35	7 153.75	11.91	9.08	76.69	7 275.76
89_pegase	8.04	6.32	63.66	6 681.22	18.55	16.40	50.00	7 221.67	30.78	29.85	94.44	6 806.40
118_ieee	22.41	17.44	49.36	7 285.80	20.69	13.60	50.42	7 210.12	21.05	15.87	50.21	7 258.33
162_ieee_dtc	37.65	36.23	93.67	7 228.76	38.78	36.80	91.98	7 147.03	33.09	30.38	85.80	7 220.62
189_edin	43.75	42.32	90.53	7 075.34	18.14	15.28	49.34	7 201.87	17.79	16.22	50.00	7 209.95
300_ieee	39.20	35.08	90.71	7 230.51	37.52	35.51	88.16	7 188.88	35.59	33.83	88.90	7 220.90

5.4. Full Discrete. We now present the results of Algorithm 2 for the full discrete AC OPF. This problem includes generator and transmission line switching together with the discrete curtailment of renewables. This, as we will see hardest among the discussed problems, has - to the best of our knowledge - not yet been discussed in the literature. We adjust the input data the same way as in Subsection 5.2 and 5.3 to generate reasonable test cases.

Table 5 depicts the corresponding results. Our method solves 11 out of 59 instances to global optimality. Two test cases are proven infeasible. Unfortunately, Algorithm 2 was not able to find any feasible solution for three instances. In total, 11 instances have a proven gap below 1% and 14 below 10%. On average, we obtain for the final optimality gap 22.98% as arithmetic and 5.16% as geometric mean. Naturally,

these problems are the most difficult to solve since they combine all discrete decisions. However, even for these very challenging optimization problems, we are able to compute solutions with a reasonable optimality gap.

TABLE 5. Results summary for the full discrete AC OPF.

nesta_case_	standard						API						SAD					
	IG (%)	FG (%)	#LO	#GO	CT (%)	T (s)	IG (%)	FG (%)	#LO	#GO	CT (%)	T (s)	IG (%)	FG (%)	#LO	#GO	CT (%)	T (s)
3_lmbd	infeas.	infeas.	0	0	0.00	2.47	15.11	0.01	0	0	81.25	32.03	infeas.	infeas.	0	0	0.00	2.58
4_gs	0.01	0.01	0	1	62.50	17.53	17.70	0.01	0	0	81.25	161.71	0.10	0.01	0	1	62.50	5.75
5_pjm	4.22	0.01	0	3	54.17	7290.54	0.23	0.01	0	2	75.00	394.52	4.16	0.01	0	2	62.50	93.78
6_ww	0.36	0.01	2	1	75.00	283.36							0.01	0.01	2	1	75.00	321.22
6_c	18.80	2.67	1	1	54.17	7293.61	17.82	0.01	0	1	62.50	1029.93	18.84	0.01	0	1	62.50	3668.15
9_wscc	10.29	9.69	3	2	57.50	7285.08	11.46	9.84	1	2	57.50	7231.04	13.25	12.84	2	2	62.50	7258.54
14_ieee	22.06	19.87	2	1	57.14	7166.12	21.80	19.02	1	1	55.36	7178.35	38.23	21.12	5	1	60.71	7096.10
24_ieee_rts	30.37	16.81	4	18	68.75	7202.15	24.19	12.34	2	22	65.63	7244.10	32.39	22.76	2	13	77.08	7270.62
29_edin	22.79	17.34	10	49	60.00	6901.41	21.29	15.06	0	5	85.83	7210.87	11.78	11.75	39	49	59.17	7284.00
30_as	43.95	22.86	0	3	61.67	7298.97	40.43	32.02	0	0	77.50	7035.66	42.29	42.00	0	0	95.00	7000.73
30_ieee	45.73	36.55	0	0	79.17	7251.24	48.45	44.67	0	0	85.83	7297.71	20.46	20.38	10	1	54.17	7298.74
30_fsr	41.17	27.82	0	2	62.50	7195.53	44.99	21.53	6	4	56.66	7112.79	45.40	35.71	3	2	78.34	7296.47
39_epri	36.05	35.00	0	0	94.37	7104.41	25.55	14.33	1	3	64.38	7297.52	33.98	33.97	0	0	92.50	7231.75
57_ieee	46.71	45.50	0	0	93.97	7133.02	50.68	47.78	1	0	91.81	7071.31	44.49	43.41	0	0	93.97	7146.65
73_ieee_rts	30.91	29.86	0	14	92.91	7233.45	27.15	25.29	0	43	79.73	7264.07	33.39	33.02	0	8	94.93	7261.94
89_pegase	38.97	38.60	0	0	92.36	6982.46	41.53	41.41	0	0	94.44	7172.11	42.39	38.87	0	0	93.06	6474.09
118_ieee	45.73	44.79	0	0	92.58	7213.77	41.46	37.53	0	0	85.80	7082.23	47.71	46.45	0	0	95.34	7218.47
162_ieee_dtc	39.13	36.05	0	0	94.91	7216.56	40.26	37.21	0	0	94.60	7204.50	36.98	35.79	0	0	94.60	7233.21
189_edin	no sol.	no sol.	0	0	0.00	2633.07	no sol.	no sol.	0	0	0.00	2640.53	no sol.	no sol.	0	0	0.00	2618.90
300_ieee	36.72	34.88	0	0	92.52	6959.67	36.23	33.38	0	0	89.23	7256.31	39.32	32.98	0	0	88.98	7203.86

5.5. Results at Short Run Time. In addition to the question of how good solutions are obtained with no or large time limit, it is also relevant which solution quality is to be expected for a short run time. In Table 6, we give an overview of the average optimality gaps provided by our method for the five different models after a run time of 15 minutes and two hours. The overview shows that our approach is able to find feasible solutions with a high quality after a relatively short time. In many cases the main computational run time is needed to strengthen the dual bound in order to prove optimality.

TABLE 6. Average gap (arithmetic and geometric mean) reported after a run time of 15 minutes and 2 hours for different models.

	arithmetic mean		geometric mean	
	15min	2h	15min	2h
transmission line switching (3.1)	4.19%	1.53%	0.30%	0.16%
generator switching (3.2)	6.97%	2.63%	0.33%	0.19%
curtailment (3.3)	16.9%	13.79%	2.61%	2.19%
full discrete (5.4)	26.64%	22.98%	7.44%	5.16%

5.6. Effect of the Algorithmic Enhancements. In this Subsection, we examine the effect of the algorithmic enhancements of Section 4.2 on the performance of Algorithm 2. To this end, we repeat the numerical experiments for the full discrete instances, while skipping one of the extensions of the algorithm each time. We focus on these instances because they are the most challenging for our approach. We measure the average final optimality gap that is achieved by omitting the improvements from Section 4.2 and show the number of instances where a feasible solution could be found during preprocessing (start) and after termination (end). Since it is not always possible to find a solution for every instance, we calculate the average gap of the 47 test cases from 59 for which solutions could be found after termination even without

enhancements. Table 7 displays the effect of the algorithmic improvements. Please note that for consistency, we have indicated both arithmetic and geometric means. However, since the arithmetic mean is strongly influenced by very large outliers, we measure the effects of an enhancement from Section 4.2 preferable using the geometric mean.

TABLE 7. Effect of the algorithmic enhancements on the number of instances where no solution was found after the first iteration (start) and after termination (end) as well as on the final gap measured with arithmetic and geometric mean.

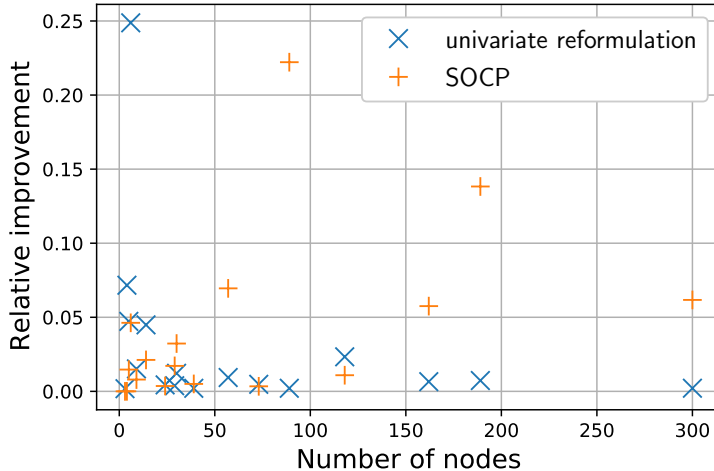
Algorithm 2...	#no sol.		final gap	
	start	end	arithm.	geom.
with all extensions (4.2)	3	3	22.02%	4.79%
without bound tightening (4.2.1)	7	7	22.52%	4.77%
without univariate reformulation (4.2.2)	7	5	26.78%	15.89%
without lower cuts (4.2.3)	4	4	21.86%	5.36%
without refinement strategy (4.2.4)	3	3	22.25%	5.47%
without no-good cuts (4.2.5)	3	3	22.42%	4.90%
without SOCP (4.2.6)	3	3	20.75%	6.10%
without outer approximation (4.2.7)	4	4	22.54%	4.80%
without DC heuristic (4.2.8)	44	3	23.74%	5.11%
without curtailment cuts (4.2.9)	4	4	21.51%	5.33%

We can see that the number of cases in which no solution was found varies. For example, without bound tightening from Section 4.2.1 it is not possible to find a feasible solution for seven instances instead of three. The univariate reformulation of bilinear products in combination with the McCormick constraints has by far the largest impact on the solution quality. By reducing the number of binaries with a comparable approximation quality, the run time of Algorithm 2 is shortened and therefore more iterations are performed in the same time. The SOCP constraints (4.2.6) and the DC heuristic (4.2.8) also contribute significantly to the performance of our approach. These improvements are most noticeable, because already the first relaxation is strongly enhanced by tighter primal and dual bounds. All other enhancements from Section 4.2 increase the solution quality only by a smaller proportion.

Finally, we compare the performance scalability of the two best enhancements: the univariate reformulation of bilinear products in combination with the McCormick constraints and the SOCP constraints (4.2.6). Figure 3 depicts the relative improvement on dual bounds in dependence of network size after a run time limit of 2 hours.

As the network size increases, the benefit of the univariate reformulation seems to decrease dramatically, while the benefit of the SOCP constraints (4.2.6) increases slightly. This phenomenon can be explained as follows. During the solution of the MISOCP relaxations in Algorithm 2, the advantage of the SOCP constraints (4.2.6) is apparent from the first node in the branch-and-cut tree. In contrast, the univariate reformulation results in fewer binary variables and thus generally requires fewer branching steps to solve the MISOCP relaxations. However, to capture the advantage of the univariate reformulation, a certain number of branching steps is required. This

FIGURE 3. Average relative improvement of the univariate reformulation of bilinear products and SOCP relaxation on dual bounds in dependence of network size after a run time limit of 2 hours.



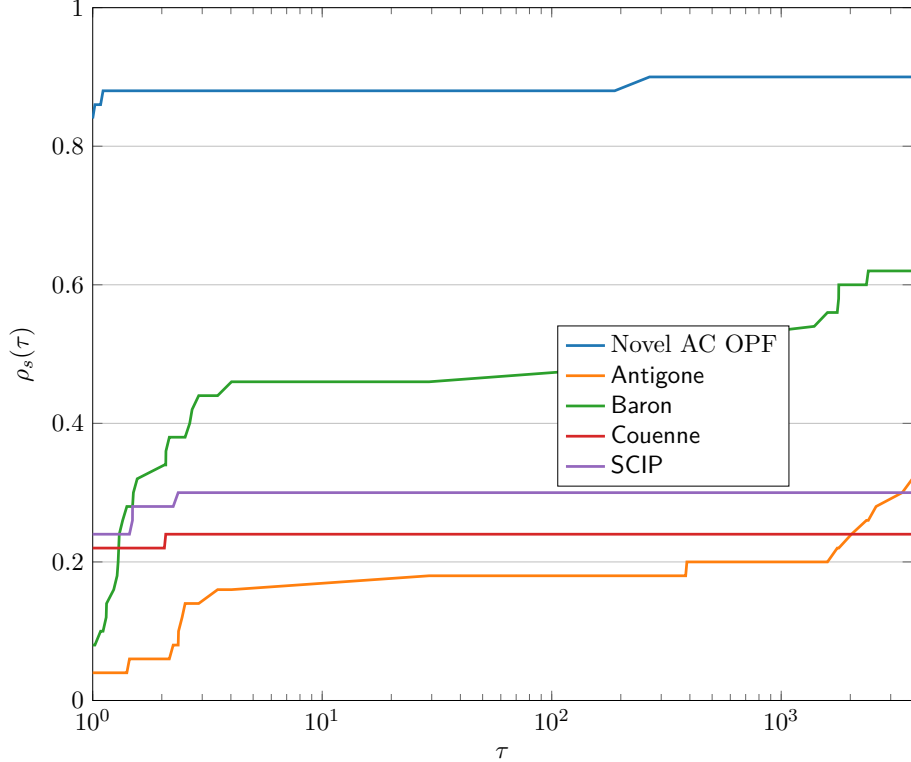
number grows as the network size increases, and consequently a higher run time limit is needed to benefit from the univariate reformulation.

5.7. Comparison with other MINLP Solvers. In this part, we use the same NESTA instances as in the full discrete case to compare our approach more extensively with state-of-the-art MINLP solvers. Since most MINLP solvers do not support trigonometric functions, we use the rectangular model that we describe in the Appendix 8. We utilize as such solvers Antigone 1.1, Baron 20.10.16, and SCIP 7.0, all again within GAMS 33.2.0. For the solver Couenne 0.5, we used GAMS 31.2.0. Note that for a fair comparison, the MINLP/MIQCP solvers also have 4 cores available and run in parallel.

We compare relative optimality gaps (see formula (18)) using performance profiles as proposed by [19]. Let $g_{p,s}$ be the best gap obtained by solver s for problem p after a certain time limit. With the performance ratio $r_{p,s} = g_{p,s} / \min_s g_{p,s}$, the performance profile $\rho_s(\tau)$ is the percentage of problems solved by approach s such that the ratios $r_{p,s}$ are within a factor $\tau \in \mathbb{R}$ of the best possible ratios. An instance is considered to be solved as soon as the gap is less than 0.0001, which is the default value of most solvers. For the performance profile, we set $g_{p,s} = 0.0001$ for solved instances to prevent a division by zero. All performance profiles are generated with the help of Perprof-py; see [50].

Figure 4 compares relative optimality gaps for the rectangular version of the discrete AC OPF problem from Section 5.4 performed on the NESTA instances. We can clearly see that our method outperforms all other state-of-the-art MINLP solvers. In more than 80% of all cases, we obtain the tightest gaps with our approach. Furthermore, we find feasible solutions for roughly 90% of all instances. All other solvers yield the best gaps for less than about 25% of all cases. Regarding feasible solutions, Baron

FIGURE 4. Performance profile for our method (Novel AC OPF), Antigone, Baron, Couenne, and SCIP comparing relative optimality gaps obtained after a run time limit of 2 hours for the rectangular model from Appendix 8.



is the best of the MINLP solvers and computes solutions for roughly 60% of the instances.

To gain a better understanding of the performance profile in Figure 4 that compares relative optimality gaps, we separately compare both primal and dual bounds in Figure 5. In case of primal bounds, $g_{p,s}$ is now the best objective value corresponding to the best feasible solution obtained by solver s for problem p after a certain time limit. For dual bounds, we define $g_{p,s} := 1/d_{p,s}$, where $d_{p,s}$ is the best dual bound found by solver s for problem p .

As we can see, our method delivers by far the best primal bounds. With the exception of Baron, all other MINLP solvers struggle even to find feasible solutions. Our approach also yields the tightest dual bounds, while all other MINLP solvers compute dual bounds that are roughly 30% weaker than ours. In conclusion, our method provides the best gaps because it finds by far the best feasible solutions and delivers the tightest dual bounds.

Finally, we perform a comparison of our approach to state-of-the-art MINLP solvers on the basis of the extended conic quadratic formulation from Section 2. To this end, we relax the involved trigonometric functions due to the non-compatibility of classical MINLP solvers with trigonometric terms. We replace these terms with

a piecewise linear relaxation that consists of one simplex for each trigonometric function as in Section 4.1. Consequently, we obtain for each problem instance a mixed-integer quadratically constrained program (MIQCP) that we use for the comparison. The approximation of the trigonometric expressions are not further refined in the experiments of this section. Please note, that in addition to the experiments at the beginning of this subsection, we now include Gurobi 9.1.0 within GAMS 33.2.0 to the set of MINLP solvers, since it is capable of solving the corresponding MIQCP problems.

Figure 6 compares relative optimality gaps for the MIQCP relaxation of the full discrete AC OPF problem from Section 5.4 performed on the 59 NESTA instances. We see a very similar picture to the one in the comparison based on the rectangular formulation. In about 70 % of all cases, we obtain the tightest gaps with our approach and we find feasible solutions for roughly 90 % of all instances.

To obtain a more in-depth look at the gaps, we again separately compare both primal and dual bounds in Figure 7. As in the comparison with the rectangular formulation, our method computes significantly better primal bounds. Baron manages to find comparatively good feasible solutions, followed by Antigone in third place. All other MINLP solvers again struggle to find any feasible solutions. Compared to the rectangular model, the performance of the MINLP solvers is somewhat better with respect to dual bounds. SCIP yields approximately the same bounds as our approach, with Gurobi in third place. All other MINLP solvers, however, deliver dual bounds that are about 40 % weaker than ours. Altogether, our method again computes the best gaps since it finds by far the best feasible solutions and delivers dual bounds that are among the tightest.

Additionally, the constructed MIQCP problems in this subsection are very similar to the full discrete AC OPF problems from Subsection 5.4 as our approach delivers very similar gaps. On average, for these MIQCPs, we obtain an optimality gap of 22.13% as arithmetic and 5.42% as geometric mean, which is almost identical to the values from Table 5. These numerical results again illustrate that the novel approach is very efficient, can solve the instances much faster than the available methods, and can be easily applied in the area of discrete AC OPF.

5.8. Discussion. In summary, the results show that our approach is very well suited to solve AC OPF with discrete decisions to global optimality. In the majority of the test cases, we are able to find high-quality solutions and reduce the optimality gap significantly. Even with a short run time, our method is capable of finding solutions of reasonable quality in most cases. For the transmission line and generator switching, the difficulty of the problem seems to be dominated by the NLP part, since adding the SOCP constraints from Section 4.2.6 has a crucial impact on the quality of the solutions. Our method delivers comparable results to other approaches for the transmission line switching from the literature.

The incorporation of the discrete curtailment, however, immensely affects the overall difficulty. For these cases, it is more challenging to find reasonable integer-feasible solutions and the convex SOCP relaxation is not as tight as in the other cases. This indicates that the complexity of these problems shifts from the NLP part to the discrete part. As mentioned before, our relaxation approach preserves the discrete structure of the problem. It turns out that the relaxation solutions allows us to find

integer-feasible solutions more easily since we can utilize mature MIP technology to obtain very good starting values for a local NLP search. Without these starting values it may be difficult to find feasible MINLP solutions at all. This claim is supported by the promising numerical results for the full discrete AC OPF problem and the comparison with state-of-the-art MINLP solvers for the rectangular formulation and the MIQCP relaxation of the extended conic quadratic formulation.

Our framework can be further extended to different applications like unit commitment problems with AC OPF constraints. The discrete curtailment instances can be seen as an example for general electricity network problems with discrete generator feed-in. We have covered an example of this with the curtailment of renewables, which is being implemented in discrete steps in Germany under the Renewable Energy Sources Act (EEG). With transmission line switching, we can also model network expansion problems, where typically for each line an extension is possible in a certain number of given modules which leads to discrete decisions in the flavor of the tasks studied here.

6. CONCLUSION

In this paper, we presented a general purpose approach for solving AC OPF problems with discrete decision to global optimality. It is based on the MINLP solution framework proposed in [11] that essentially solves an MINLP by solving a series of MIP relaxations and has been used successfully in the context of gas network optimization. We enhanced this method by both general and problem specific extensions, while maintaining convergence to an global optimum. In this regard, the univariate reformulation of bivariate terms and the SOCP constraints of the extended conic quadratic AC OPF model delivered the most benefit.

We presented models for incorporating discrete decisions and demonstrated the applicability of our approach by extensive numerical results. Furthermore, we observed that different discrete decisions are associated with varying degrees of difficulty, while the problems with the discrete curtailment of renewables poses by far the greatest challenge. In many cases, our method was able to find near-global optimal solutions. Even with a short run time, it delivered high-quality solutions in most cases. Our approach preserves the discrete structure of the problem, while it only relaxes its nonlinearities. Consequently, the discrete part of the problem is essentially tackled by mature MIP technology. We therefore believe that our solution framework is suitable for AC OPF problems with various types of discrete decisions, including those that are not covered in this paper.

There is, of course, still room for improvements. Besides a more sophisticated preprocessing or further heuristic approaches, we believe that the combination of several relaxation techniques is a very promising direction to further improve the solution of optimization problems in power system analysis.

7. ACKNOWLEDGEMENTS

We want to thank the anonymous reviewers for their very valuable comments that helped to improve and clarify this manuscript. This research has been funded by the Federal Ministry of Education and Research of Germany (grant 05M18WEB). This research has been performed as part of the Energie Campus Nürnberg and is

supported by funding of the Bavarian State Government. We would like to thank the "Deutsche Forschungsgemeinschaft" (DFG) for their support within projects A05, B06, B07 and B10 of the Sonderforschungsbereich/Transregio 154 "Mathematical Modelling, Simulation and Optimization using the Example of Gas Networks". This work has been supported by grant 03El1036A from the Federal Ministry for Economic Affairs and Energy, Germany.

REFERENCES

- [1] A. Bärmann, F. Liers, A. Martin, M. Merkert, C. Thurner, and D. Weninger. "Solving network design problems via iterative aggregation". In: *Mathematical Programming Computation* 7 (2015), pp. 189–217. DOI: [10.1007/s12532-015-0079-1](https://doi.org/10.1007/s12532-015-0079-1).
- [2] K.-M. Aigner, J.-P. Clarner, F. Liers, and A. Martin. *Robust approximation of chance constrained DC optimal power flow under decision-dependent uncertainty*. 2020. URL: <https://opus4.kobv.de/opus4-trr154/frontdoor/index/index/docId/312>.
- [3] ARPA-E. *Grid optimization competition*. 2018. URL: <https://gocompetition.energy.gov/>.
- [4] X. Bai, H. Weihua, K. Fujisawa, and Y. Wang. "Semidefinite programming for optimal power flow problems". In: *International Journal of Electrical Power & Energy Systems* 30 (July 2008), pp. 383–392. DOI: [10.1016/j.ijepes.2007.12.003](https://doi.org/10.1016/j.ijepes.2007.12.003).
- [5] Y. Bai, H. Zhong, Q. Xia, and C. Kang. "A Two-Level Approach to AC Optimal Transmission Switching with an Accelerating Technique". In: *IEEE Transactions on Power Systems* 32 (Jan. 2016), pp. 1–1. DOI: [10.1109/TPWRS.2016.2582214](https://doi.org/10.1109/TPWRS.2016.2582214).
- [6] E. Balas and R. Jeroslow. "Canonical Cuts on the Unit Hypercube". In: *SIAM Journal on Applied Mathematics* 23.1 (1972), pp. 61–69. DOI: [10.1137/0123007](https://doi.org/10.1137/0123007). eprint: <https://doi.org/10.1137/0123007>. URL: <https://doi.org/10.1137/0123007>.
- [7] D. Bienstock, M. Chertkov, and S. Harnett. "Chance-constrained optimal power flow: Risk-aware network control under uncertainty". In: *Siam Review* 56.3 (2014), pp. 461–495.
- [8] D. Bienstock, M. Escobar, C. Gentile, and L. Liberti. *Mathematical Programming formulations for the Alternating Current Optimal Power Flow problem*. 2020. arXiv: [2007.05334 \[math.OC\]](https://arxiv.org/abs/2007.05334).
- [9] D. Bienstock and A. Verma. "Strong NP-hardness of AC power flows feasibility". In: *Operations Research Letters* (Dec. 2015). DOI: [10.1016/j.orl.2019.08.009](https://doi.org/10.1016/j.orl.2019.08.009).
- [10] R. Burlacu, H. Egger, M. Groß, A. Martin, M. E. Pfetsch, L. Schewe, M. Sirvent, and M. Skutella. "Maximizing the storage capacity of gas networks: a global MINLP approach". In: *Optimization and Engineering* 20 (2019), pp. 543–573. DOI: [10.1007/s11081-018-9414-5](https://doi.org/10.1007/s11081-018-9414-5).

- [11] R. Burlacu, B. Geißler, and L. Schewe. “Solving mixed-integer nonlinear programmes using adaptively refined mixed-integer linear programmes”. In: *Optimization Methods and Software* 35.1 (2020), pp. 37–64. DOI: [10.1080/10556788.2018.1556661](https://doi.org/10.1080/10556788.2018.1556661).
- [12] J. Carpentier. “Contribution a l’etude du dispatching economique”. In: *Bull. Soc. Francaise Electriciens* 8 (1962), pp. 431–447.
- [13] A. Castillo, C. Laird, C. A. Silva-Monroy, J. Watson, and R. P. O’Neill. “The Unit Commitment Problem With AC Optimal Power Flow Constraints”. In: *IEEE Transactions on Power Systems* 31.6 (Nov. 2016), pp. 4853–4866. DOI: [10.1109/TPWRS.2015.2511010](https://doi.org/10.1109/TPWRS.2015.2511010).
- [14] R. D. Christie, B. F. Wollenberg, and I. Wangensteen. “Transmission management in the deregulated environment”. In: *Proceedings of the IEEE* 88.2 (2000), pp. 170–195.
- [15] C. Coffrin, H. L. Hijazi, and P. Van Hentenryck. “The QC Relaxation: A Theoretical and Computational Study on Optimal Power Flow”. In: *IEEE Transactions on Power Systems* 31.4 (July 2016), pp. 3008–3018. DOI: [10.1109/TPWRS.2015.2463111](https://doi.org/10.1109/TPWRS.2015.2463111).
- [16] C. Coffrin, D. Gordon, and P. Scott. “NESTA, The NICTA Energy System Test Case Archive”. In: *CoRR* abs/1411.0359 (2014). arXiv: [1411.0359](https://arxiv.org/abs/1411.0359). URL: <http://arxiv.org/abs/1411.0359>.
- [17] C. M. Correa-Posada and P. Sánchez-Martín. “Gas Network Optimization: A comparison of Piecewise Linear Models”. Oct. 2014. URL: http://www.optimization-online.org/DB_HTML/2014/10/4580.html.
- [18] C. D’Ambrosio, A. Lodi, S. Wiese, and C. Bragalli. “Mathematical programming techniques in water network optimization”. In: *European Journal of Operational Research* 243.3 (2015), pp. 774–788. DOI: <https://doi.org/10.1016/j.ejor.2014.12.039>. URL: <http://www.sciencedirect.com/science/article/pii/S0377221714010571>.
- [19] E. D. Dolan and J. J. Moré. “Benchmarking optimization software with performance profiles”. In: *Mathematical Programming* 91.2 (2002), pp. 201–213. DOI: [10.1007/s101070100263](https://doi.org/10.1007/s101070100263).
- [20] P. Domschke, B. Geißler, O. Kolb, J. Lang, A. Martin, and A. Morsi. “Combination of Nonlinear and Linear Optimization of Transient Gas Networks”. In: *INFORMS Journal on Computing* 23.4 (2011), pp. 605–617. DOI: [10.1287/ijoc.1100.0429](https://doi.org/10.1287/ijoc.1100.0429).
- [21] S. Frank, I. Steponavice, and S. Rebennack. “Optimal power flow: a bibliographic survey I”. In: *Energy Systems* 3 (Sept. 2012). DOI: [10.1007/s12667-012-0056-y](https://doi.org/10.1007/s12667-012-0056-y).
- [22] S. Frank, I. Steponavice, and S. Rebennack. “Optimal power flow: a bibliographic survey II”. In: *Energy Systems* 3 (Sept. 2012). DOI: [10.1007/s12667-012-0057-x](https://doi.org/10.1007/s12667-012-0057-x).
- [23] C. Gambella, J. Marecek, M. Mevissen, J. Fernández Ortega, S. Djukic, and M. Pezic. “Transmission-Constrained Unit Commitment”. In: June 2018.
- [24] GAMS. *General Algebraic Modeling System (GAMS) Release 31.2.0*. Washington, DC, USA. 2020. URL: <http://www.gams.com/>.

- [25] B. Geißler. “Towards Globally Optimal Solutions of MINLPs by Discretization Techniques with Applications in Gas Network Optimization”. PhD thesis. FAU Erlangen-Nürnberg, 2011.
- [26] A. Gleixner, T. Berthold, B. Müller, and S. Weltge. “Three Enhancements for Optimization-Based Bound Tightening”. In: *Journal of Global Optimization* 67.4 (2017), pp. 731–757. DOI: [10.1007/s10898-016-0450-4](https://doi.org/10.1007/s10898-016-0450-4).
- [27] S. Gopinath, H. Hijazi, T. Weisser, H. Nagarajan, M. Yetkin, K. Sundar, and R. Bent. “Proving global optimality of ACOPF solutions”. In: *Electric Power Systems Research* 189 (2020), p. 106688. DOI: <https://doi.org/10.1016/j.epsr.2020.106688>. URL: <https://www.sciencedirect.com/science/article/pii/S0378779620304910>.
- [28] V. Grimm, T. Kleinert, F. Liers, M. Schmidt, and G. Zöttl. “Optimal price zones of electricity markets: a mixed-integer multilevel model and global solution approaches”. In: *Optimization Methods and Software* 34.2 (2019), pp. 406–436. DOI: [10.1080/10556788.2017.1401069](https://doi.org/10.1080/10556788.2017.1401069). eprint: <https://doi.org/10.1080/10556788.2017.1401069>. URL: <https://doi.org/10.1080/10556788.2017.1401069>.
- [29] M. Gugat, G. Leugering, A. Martin, M. Schmidt, M. Sirvent, and D. Wintergerst. “Towards simulation based mixed-integer optimization with differential equations”. In: *Networks* (2018). DOI: [10.1002/net.21812](https://doi.org/10.1002/net.21812).
- [30] L. Gurobi Optimization. *Gurobi Optimizer Reference Manual*. 2020. URL: <http://www.gurobi.com>.
- [31] H. Hijazi, C. Coffrin, and P. Van Hentenryck. “Convex Quadratic Relaxations of Mixed-Integer Nonlinear Programs in Power Systems”. In: *submitted* (Jan. 2013). DOI: [10.1007/s12532-016-0112-z](https://doi.org/10.1007/s12532-016-0112-z).
- [32] R. A. Jabr. “Optimal Power Flow Using an Extended Conic Quadratic Formulation”. In: *IEEE Transactions on Power Systems* 23.3 (Aug. 2008), pp. 1000–1008. DOI: [10.1109/TPWRS.2008.926439](https://doi.org/10.1109/TPWRS.2008.926439).
- [33] R. A. Jabr. “Radial distribution load flow using conic programming”. In: *IEEE Transactions on Power Systems* 21.3 (2006), pp. 1458–1459. DOI: [10.1109/TPWRS.2006.879234](https://doi.org/10.1109/TPWRS.2006.879234).
- [34] B. Kocuk, S. S. Dey, and X. A. Sun. “New Formulation and Strong MISOCP Relaxations for AC Optimal Transmission Switching Problem”. In: *IEEE Transactions on Power Systems* 32.6 (Nov. 2017), pp. 4161–4170. DOI: [10.1109/TPWRS.2017.2666718](https://doi.org/10.1109/TPWRS.2017.2666718).
- [35] B. Kocuk, S. Dey, and X. Sun. “Strong SOCP Relaxations for the Optimal Power Flow Problem”. In: *Operations Research* 64.6 (2016), pp. 1177–1196. DOI: [10.1287/opre.2016.1489](https://doi.org/10.1287/opre.2016.1489).
- [36] B. Kocuk, S. S. Dey, and X. A. Sun. “Matrix minor reformulation and SOCP-based spatial branch-and-cut method for the AC optimal power flow problem”. In: *Mathematical Programming Computation* 10.4 (Dec. 2018), pp. 557–596. DOI: [10.1007/s12532-018-0150-9](https://doi.org/10.1007/s12532-018-0150-9).
- [37] M. Kuchlbauer, F. Liers, and M. Stingl. “Adaptive Bundle Methods for Nonlinear Robust Optimization”. In: *INFORMS Journal on Computing* 34.4 (2022), pp. 2106–2124. DOI: [10.1287/ijoc.2021.1122](https://doi.org/10.1287/ijoc.2021.1122). eprint: <https://doi.org/10.1287/ijoc.2021.1122>.

- [org/10.1287/ijoc.2021.1122](https://doi.org/10.1287/ijoc.2021.1122). URL: <https://doi.org/10.1287/ijoc.2021.1122>.
- [38] M. Kuchlbauer, F. Liers, and M. Stingl. “Outer approximation for mixed-integer nonlinear robust optimization”. In: *Journal of Optimization Theory and Applications* (2022). URL: <https://opus4.kobv.de/opus4-trr154/frontdoor/index/index/docId/414>.
- [39] S. Kuhn. “Betrieboptimierung von elektrischen Energieerzeugungsanlagen und Übertragungssystemen bei unvollständiger Information”. PhD thesis. Universität Duisburg-Essen, 2011.
- [40] J. Liu, C. D. Laird, J. K. Scott, J.-P. Watson, and A. Castillo. “Global Solution Strategies for the Network-Constrained Unit Commitment Problem With AC Transmission Constraints”. In: *IEEE Transactions on Power Systems* 34.2 (2019), pp. 1139–1150. DOI: [10.1109/TPWRS.2018.2876127](https://doi.org/10.1109/TPWRS.2018.2876127).
- [41] M. Lu, H. Nagarajan, R. Bent, S. D. Eksioglu, and S. J. Mason. “Tight Piecewise Convex Relaxations for Global Optimization of Optimal Power Flow”. In: *2018 Power Systems Computation Conference (PSCC)*. 2018, pp. 1–7. DOI: [10.23919/PSCC.2018.8442456](https://doi.org/10.23919/PSCC.2018.8442456).
- [42] S. J. Maher, T. Fischer, T. Gally, G. Gamrath, A. Gleixner, R. L. Gottwald, G. Hendel, T. Koch, M. E. Lübbecke, M. Miltenberger, B. Müller, M. E. Pfetsch, C. Puchert, D. Rehfeldt, S. Schenker, R. Schwarz, F. Serrano, Y. Shinano, D. Weninger, J. T. Witt, and J. Witzig. *The SCIP Optimization Suite 4.0*. Tech. rep. 17-12. Takustr. 7, 14195 Berlin: ZIB, 2017. URL: <https://opus4.kobv.de/opus4-zib/frontdoor/index/index/docId/6217> (visited on 03/01/2019).
- [43] A. Mary, B. Cain, and R. O’Neill. “History of optimal power flow and formulations”. In: *Fed. Energy Regul. Comm.* 1 (Jan. 2012), pp. 1–36.
- [44] G. P. McCormick. “Computability of Global Solutions to Factorable Nonconvex Programs: Part I – Convex Underestimating Problems”. In: *Math. Program.* 10.1 (Dec. 1976), pp. 147–175. DOI: [10.1007/BF01580665](https://doi.org/10.1007/BF01580665). URL: <https://doi.org/10.1007/BF01580665>.
- [45] A. Morsi. “Solving MINLPs on Loosely-Coupled Networks with Applications in Water and Gas Network Optimization”. PhD thesis. Friedrich-Alexander-Universität Erlangen-Nürnberg (FAU), 2013.
- [46] G. Nannicini and P. Belotti. “Rounding-based heuristics for nonconvex MINLPs”. In: *Mathematical Programming Computation* 4 (Mar. 2012), pp. 1–31. DOI: [10.1007/s12532-011-0032-x](https://doi.org/10.1007/s12532-011-0032-x).
- [47] K. Purchala, L. Meeus, D. V. Dommelen, and R. Belmans. “Usefulness of DC power flow for active power flow analysis”. In: *IEEE Power Engineering Society General Meeting, 2005*. June 2005, 454–459 Vol. 1. DOI: [10.1109/PES.2005.1489581](https://doi.org/10.1109/PES.2005.1489581).
- [48] E. Salgado, A. Scozzari, F. Tardella, and L. Liberti. “Alternating Current Optimal Power Flow with Generator Selection”. In: *Combinatorial Optimization*. Ed. by J. Lee, G. Rinaldi, and A. R. Mahjoub. Springer International Publishing, 2018, pp. 364–375.

- [49] B. Saravanan, S. Das, S. Sikri, and D. P. Kothari. “A solution to the unit commitment problem—a review”. In: *Frontiers in Energy* 7.2 (June 2013), pp. 223–236. DOI: [10.1007/s11708-013-0240-3](https://doi.org/10.1007/s11708-013-0240-3).
- [50] A. Siqueira, R. Gaia Costa da Silva, and L.-R. Santos. “Perprof-py: A Python Package for Performance Profile of Mathematical Optimization Software”. In: *Journal of Open Research Software* 4 (Apr. 2016). DOI: [10.5334/jors.81](https://doi.org/10.5334/jors.81).
- [51] M. Tawarmalani and N. V. Sahinidis. “A polyhedral branch-and-cut approach to global optimization”. In: *Mathematical Programming* 103 (2 2005), pp. 225–249.
- [52] B. Vieira, S. Mayerle, L. Campos, and L. Coelho. “Optimizing drinking water distribution system operations”. In: *European Journal of Operational Research* 280 (Aug. 2019). DOI: [10.1016/j.ejor.2019.07.060](https://doi.org/10.1016/j.ejor.2019.07.060).
- [53] J. P. Vielma, S. Ahmed, and G. L. Nemhauser. “Mixed-Integer Models for Non-separable Piecewise-Linear Optimization: Unifying Framework and Extensions”. In: *Operations Research* 58.2 (2010), pp. 303–315. DOI: [10.1287/opre.1090.0721](https://doi.org/10.1287/opre.1090.0721).
- [54] Zhifeng Qiu, G. Deconinck, and R. Belmans. “A literature survey of Optimal Power Flow problems in the electricity market context”. In: *2009 IEEE/PES Power Systems Conference and Exposition*. 2009, pp. 1–6.

8. RECTANGULAR FORMULATION

8.1. The AC OPF Model. The complex voltage on a bus $k \in B$ is given by $V_k = e_k + if_k$, where $e_k = \Re(V_k)$ is the real part of the voltage and $f_k = \Im(V_k)$ the imaginary part, respectively. Given the extended conic quadratic formulation in Section 2.1 one express the power flow constraints in the rectangular coordinates using the reformulations

$$\begin{aligned} c_{kk} &= e_k^2 + f_k^2, \\ c_{kl} &= e_k e_l + f_k f_l, \\ t_{kl} &= e_k f_l - e_l f_k. \end{aligned}$$

We obtain the rectangular power flow constraints

$$\begin{aligned} p_k^g - \hat{p}_k^d &= g_{kk}(e_k^2 + f_k^2) + \sum_{l \in \delta(k)} p_{kl} && \text{for all } k \in B, \\ q_k^g - \hat{q}_k^d &= -b_{kk}(e_k^2 + f_k^2) + \sum_{l \in \delta(k)} q_{kl} && \text{for all } k \in B, \\ p_{kl} &= -G_{kl}(e_k^2 + f_k^2 - e_k e_l - f_k f_l) - B_{kl}(e_k f_l - e_l f_k) && \text{for all } (k, l) \in L, \\ q_{kl} &= B_{kl}(e_k^2 + f_k^2 - e_k e_l - f_k f_l) - G_{kl}(e_k f_l - e_l f_k) && \text{for all } (k, l) \in L. \end{aligned}$$

We point out that one of the variables f_k needs to be set to zero as the voltage angle at a reference node is fixed at zero. The voltage magnitude bounds (3l) can be expressed with

$$(|V_k|^-)^2 \leq e_k^2 + f_k^2 \leq (|V_k|+)^2 \quad \text{for all } k \in B.$$

We remark that $-\pi/2 < \theta_l - \theta_k < \pi/2$ holds in practice for a lot of test instances. Under this assumption, we can reformulate the voltage angle bound (3m) equivalently

by

$$\tan \theta_{kl}^- \leq \frac{e_l f_k - e_k f_l}{e_k e_l + f_k f_l} \leq \tan \theta_{kl}^+ \quad \text{for all } (k, l) \in L.$$

In conclusion, the rectangular AC OPF flow model can be formulated as

$$\begin{aligned} & \min_{p^g, q^g, e, f} \sum_{k \in U} C_k(p_k^g) \\ & \text{s.t. } p_k^g - p_k^d = g_{kk}(e_k^2 + f_k^2) + \sum_{l \in \delta(k)} p_{kl} \quad \text{for all } k \in B, \\ & q_k^g - q_k^d = -h_{kk}(e_k^2 + f_k^2) + \sum_{l \in \delta(k)} q_{kl} \quad \text{for all } k \in B, \\ & p_{kl} = -G_{kl}(e_k^2 + f_k^2 - e_k e_l - f_k f_l) - B_{kl}(e_k f_l - e_l f_k) \quad \text{for all } (k, l) \in L, \\ & q_{kl} = B_{kl}(e_k^2 + f_k^2 - e_k e_l - f_k f_l) - G_{kl}(e_k f_l - e_l f_k) \quad \text{for all } (k, l) \in L, \\ & p_{kl}^2 + q_{kl}^2 \leq (d_{kl}^+)^2 \quad \text{for all } (k, l) \in L, \\ & (p_k^g)^- \leq p_k^g \leq (p_k^g)^+ \quad \text{for all } k \in U, \\ & (q_k^g)^- \leq q_k^g \leq (q_k^g)^+ \quad \text{for all } k \in U, \\ & (|V_k|^-)^2 \leq e_k^2 + f_k^2 \leq (|V_k|^+)^2 \quad \text{for all } k \in B, \\ & \tan \theta_{kl}^-(e_k e_l + f_k f_l) \leq e_l f_k - e_k f_l \leq \tan \theta_{kl}^+(e_k e_l + f_k f_l) \quad \text{for all } (k, l) \in L, \\ & e_k e_l + f_k f_l \geq 0 \quad \text{for all } (k, l) \in L, \\ & p^g, q^g \in \mathbb{R}^{|U|}, e, f \in \mathbb{R}^{|B|}. \end{aligned}$$

8.2. Extension to Discrete Decisions. The generator switching 5.2 and the discrete curtailment of renewables 5.3 can be directly integrated into the rectangular AC OPF model. In order to model the switching of transmission lines, we follow again [34] and introduce additional variables $\tilde{c}_{kl} := c_{kk} s_{kl}^t$ for every line $(k, l) \in L$, where $s_{kl}^t \in \{0, 1\}$ denotes the switching status of a transmission line $(k, l) \in L$. The switching constraints of a line read

$$p_{kl} = -G_{kl}(\tilde{c}_{kl} - c_{kl}) - H_{kl} t_{kl}, \quad (20a)$$

$$q_{kl} = H_{kl}(\tilde{c}_{kl} - c_{kl}) - G_{kl} t_{kl}, \quad (20b)$$

$$c_{kk} = e_k^2 + f_k^2, \quad (20c)$$

$$c_{kl} = (e_k e_l + f_k f_l) s_{kl}^t, \quad (20d)$$

$$t_{kl} = (e_k f_l - e_l f_k) s_{kl}^t, \quad (20e)$$

$$\tilde{c}_{kl} = c_{kk} s_{kl}^t. \quad (20f)$$

The constraints (20d) and (20e) contain trilinear expressions involving the binary variables s_{kl}^t . With additional mixed-integer constraints (big-M reformulation) one can reduce the complexity of the nonlinearities to bivariate expressions. However, in

our numerical experiments the set of constraints (20) lead to the best results when using state-of-the-art MINLP solvers.

¹FRIEDRICH-ALEXANDER UNIVERSITÄT ERLANGEN-NÜRNBERG (FAU), DISCRETE OPTIMIZATION, CAUERSTR. 11, 91058 ERLANGEN, GERMANY

²ENERGIE CAMPUS NÜRNBERG, FÜRTH STR. 250, 90429 NÜRNBERG, GERMANY

³FRAUNHOFER INSTITUTE FOR INTEGRATED CIRCUITS IIS, NORDOSTPARK 84, 90411 NÜRNBERG, GERMANY

FIGURE 5. Performance profiles for our method (Novel AC OPF), Antigone, Baron, Couenne, and SCIP comparing primal bounds (upper) and dual bounds (lower) obtained after a run time limit of 2 hours for the rectangular model from Appendix 8.

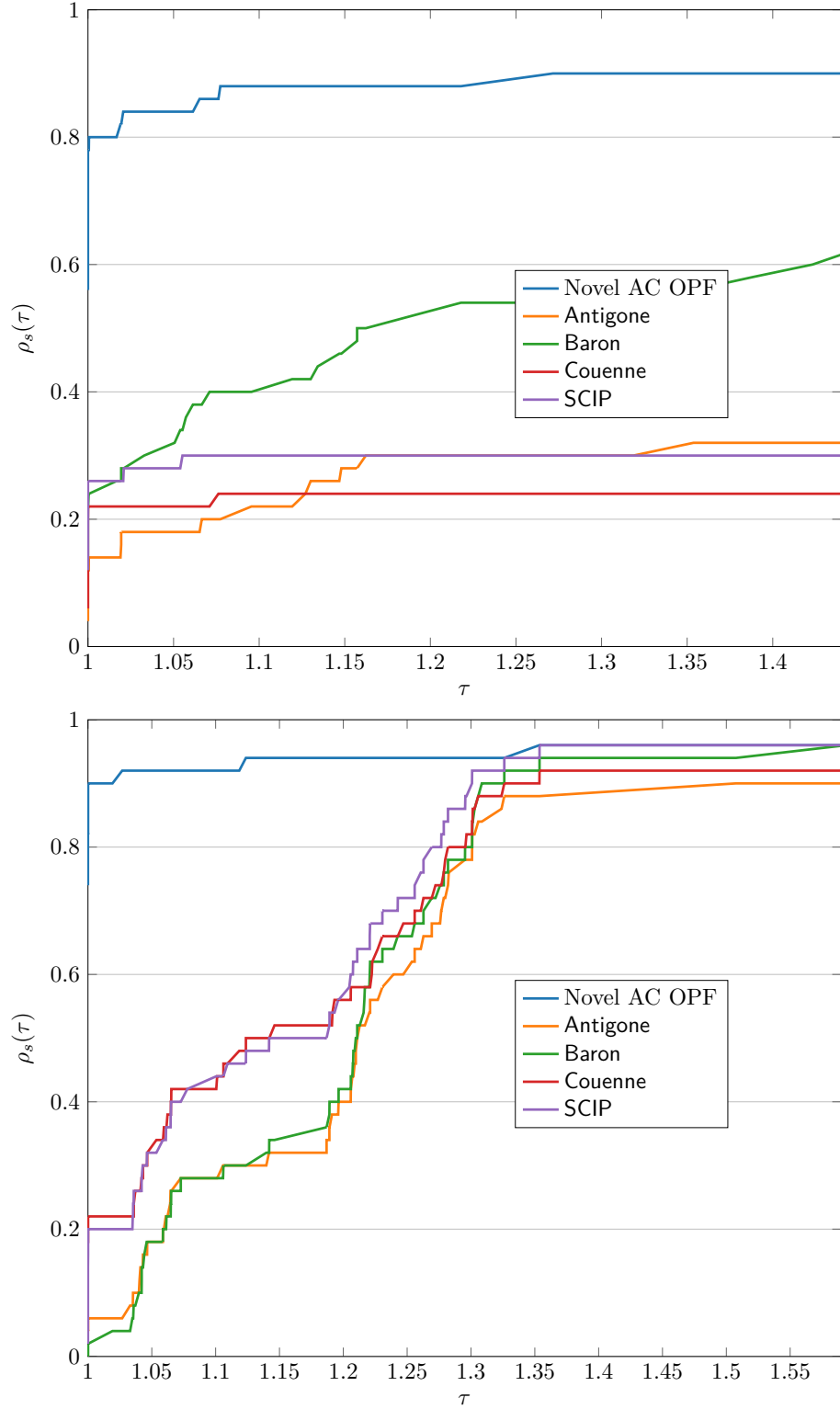


FIGURE 6. Performance profile for our method (Novel AC OPF), Antigone, Baron, Couenne, Gurobi, and SCIP comparing relative optimality gaps obtained after a run time limit of 2 hours for the extended conic quadratic formulation from Section 2.

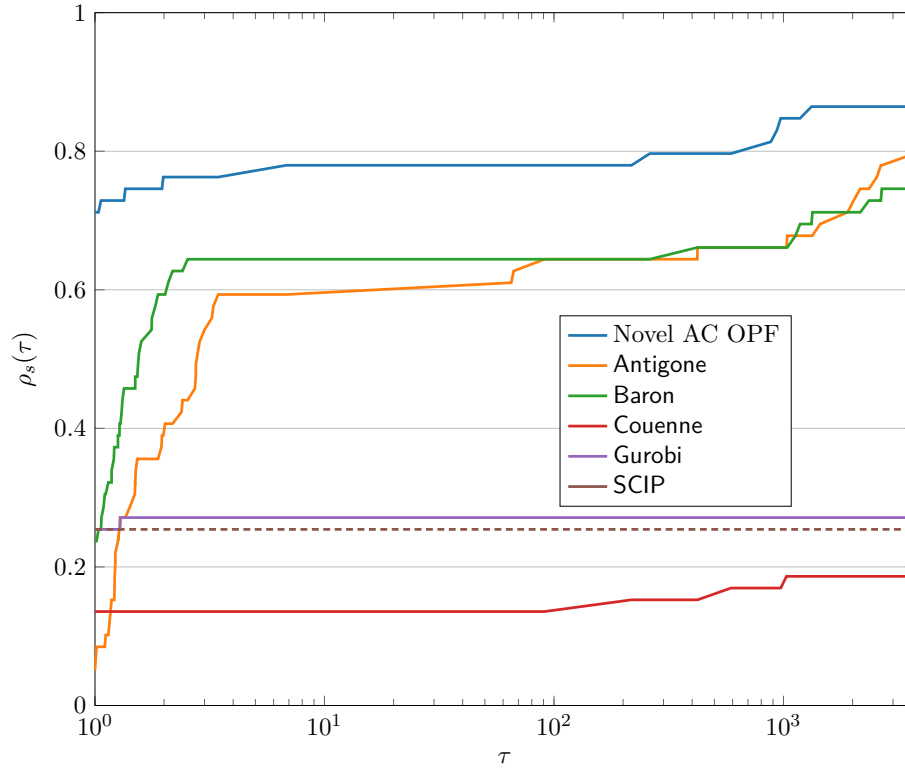


FIGURE 7. Performance profiles for our method (Novel AC OPF), Antigone, Baron, Couenne, Gurobi, and SCIP comparing primal bounds (upper) and dual bounds (lower) obtained after a run time limit of 2 hours for the extended conic quadratic formulation from Section 2.

